Molecular Hydrogen in the Cooling Flow Cluster Abell 1795

by

Louise Edwards

A THESIS SUBMITTED IN PARTIAL FULFILMENT OF
THE REQUIREMENTS FOR THE DEGREE OF

MASTER OF SCIENCE

in

Astronomy

(Department of Astronomy and Physics)

SAINT MARY'S UNIVERSITY

October 14, 2003

Your file Votre référence
ISBN: 0-612-86574-6
Our file Notre référence
ISBN: 0-612-86574-6

Contents

List of Figures

List of Tables

Acknowledgments

I would like to thank my supervisor Dr. Francine Marleau for her advice and guidance throughout this project. I would especially like to thank her for the opportunities she gave to feel like a "real" astronomer. I feel grateful that I was able to work on a project through the initial idea, observations, reduction and analysis stages. She also sent me to conferences (CFHTLS and CFC) and a workshop (SIRTF) and 2 observing trips (CFHT) which were very helpful in learning more about astronomy and in feeling like a part of the astronomical community.

I would also like to thank Dr. Gary Welch and Dr. David Guenther for taking the time to be on my oral exam committee and my thesis defense. I have felt very comfortable in the department here and the entire staff has been easy to talk to. Thank you to Gary Welch for coming to Hawaii to observe with us and to Gary Welch and David Guenther for the pep talks they gave me when I wasn't sure I wanted to continue on in research.

A thank you also goes out to Dr. Chris Loken for being my external reader. I would like to thank Dr. Nick Tothill for his help on how to reduce IR data.

Thank you Sean for reading through my thesis at various "draft" stages and giving me your opinion and friendship.

Thanks to Glenn and Ashley for all the fun nights and for listening to my project problems and sharing yours with me. I also have to thank all the other physics students who made my life in Halifax (away from Victoria) not only tolerable but enjoyable.

Abstract

An abstract of the thesis of Louise O.V. Edwards for the Master of Science in Astronomy presented August 20th, 2003.

Title: Molecular Hydtrogen in the Cooling Flow Cluster Abell 1795

A cooling flow forms in a galaxy cluster when the internal pressure of the gas drops below the gravitational potential of the cluster due to the cooling of the X-ray gas in the Inter-Cluster Medium (ICM). The cooling flow hypothesis is that the cooling X-ray gas condenses into clouds of molecular hydrogen and perhaps forms stars.

This thesis explores the above picture and is presented in two parts. First, we assemble cooling flow clusters and their X-ray properties in a study of alignments of the X-ray properties and optical emission. Second, we use that information to help pick the best cooling flow cluster in which to image the 2.12 μm v=(1-0) S(1) emission line of molecular hydrogen. We choose Abell 1795 (redshift of z=0.06) as (1) it can be imaged within our time constraints of one night on the Canada-France-Hawaii Telescope's infrared camera (CFHT-IR); (2) the line flux has previously been determined; (3) high resolution Chandra X-ray data is available; and (4) this cluster is well studied at other wavelengths.

We find the morphology of the molecular hydrogen emission in the Central Dominant Galaxy (CDG) of Abell 1795 to be condensed and compare this image to that of the CDG in other wavebands. We conclude that the molecular hydrogen is not a direct result of the cooling flow, rather it is cooler gas that has been reheated by an Active Galactic Nucleus (AGN), or hot stars in the center of the galaxy.

We also, for the first time, detect molecular hydrogen emission from galaxies neighboring the CDG. We discuss what implications these observations have for the current cooling flow theory.

Chapter 1

Introduction

1.1 Clusters of Galaxies

Galaxy clusters (and superclusters) are the largest gravitationally bound objects which have been found in the Universe. Poor clusters contain as few as fifty galaxies whereas rich clusters are found to contain up to thousands of galaxies (Carroll and Ostlie 1996) within a diameter of a few megaparsecs (Mpc). Aside from galaxies, galaxy clusters also contain an intra-cluster medium (ICM). The ICM is hot, 10^7K, and bright in X-rays. The ionized gas of the ICM makes up the majority of the observable mass of the cluster and emission lines of heavy elements are seen, suggesting some processing of the gas and a complex history. Dark matter is also a large component of clusters. It is still unknown what constitutes this dark matter, which is up to ninety percent of the mass of the cluster (Sarazin 1988).

The galaxies of a galaxy cluster are bound to the central gravitational potential, where a cD galaxy is often found.

By far the largest and most luminous class of galaxy in the universe, cD galaxies are characterized by a high density of stars in the interior and a diffuse halo of stars which can reach out beyond 1 Mpc from the center of the galaxy (Sarazin 1988).

A common hypothesis is that the cD galaxies are created by mergers or galactic

cannibalism; however, there are other possible scenarios. Because they are often found near the peak of the cluster's X-ray surface brightness, it is hypothesized that cDs are connected in some way to a cluster's cooling flow.

1.2 Cooling Flows

In the 1970's, the X-ray profiles of some clusters were shown to have a sharp spike in surface brightness towards the center, as shown in Figures 1.1 and 1.2. As the surface brightness is proportional to the gas density and the cooling time is inversely proportional to the gas density (Fabian 1994) a high surface brightness implies a high central density and a short cooling time. The ICM is expected to lose enough energy from the emission of X-rays over the lifetime of the Universe to noticeably reduce its temperature. As for any cooling gas, the pressure goes down as the temperature goes down and the ICM can no longer support its own weight. Thus the ICM contracts. This is termed a cooling flow and the last few decades have brought various explanations as to the relationship between the X-ray surface brightness profiles, the cooling of the gas and the flow itself.

In the past, it was thought that if the temperature lowered to under 2 keV (2.3×10^7 K) in the center of the cluster over a time-scale less than the Hubble time, we would be able to observe this matter "dropping out" of the ICM to form cool clouds and stars. There are observations which support this hypothesis. For example, blue light is detected in excess to what is expected from the underlying galaxy. This suggests a population of hot young stars, which is abnormal for elliptical

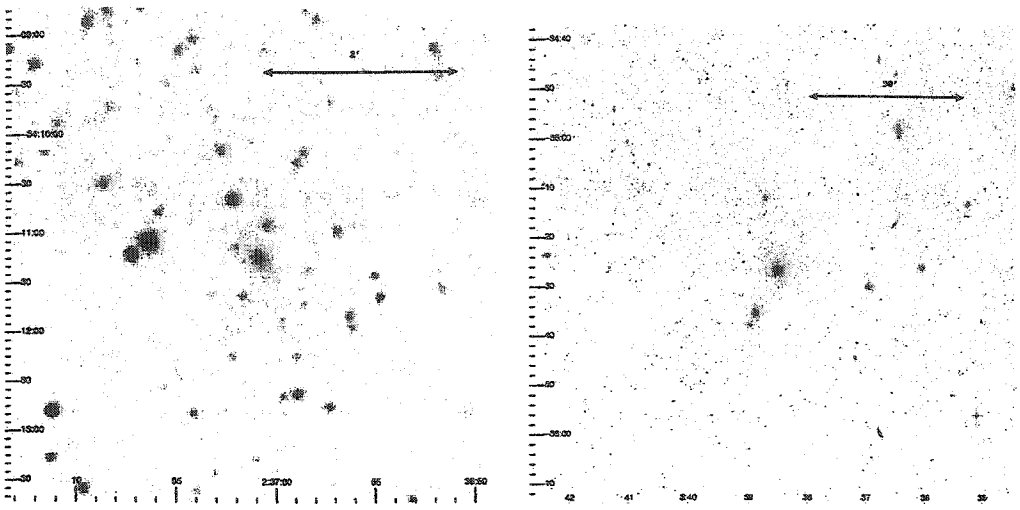

Figure 1.1: Abell 478, a cooling flow cluster is shown on the left. For comparison the center of a non-cooling flow cluster, Fornax, is shown on the right. Note that the Fornax cluster is much closer than Abell 478, and is therefore shown using a much larger scale. These are optical images from the Digital Sky Survey, the x-axis represents right ascension and the y-axis declination.

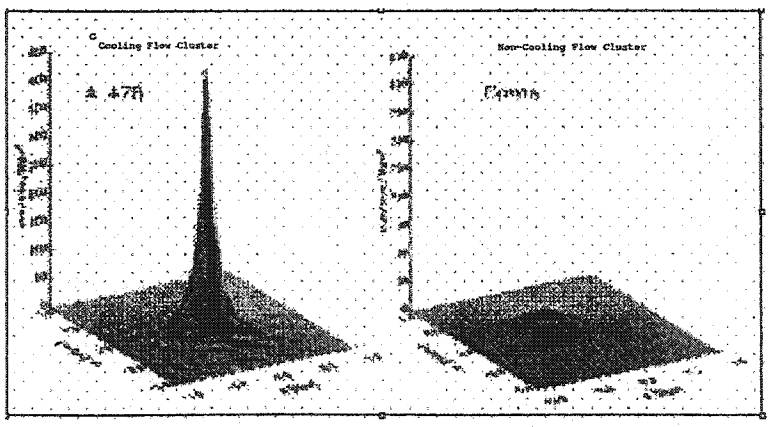

Figure 1.2: The X-ray emission of Abell 478, a cooling flow cluster, is shown on the left. A sharp increase in X-ray surface brightness (z-axis) can be seen and this is what defines a cooling flow. For comparison the X-ray emission from a non-cooling flow cluster, Fornax, is shown on the right. This figure is adapted from Fabian (2003).

galaxies.

Based on observations from X-ray observatories such as Einstein and ROSAT, large amounts of material are expected to drop out of the ICM. Mass deposition rates ($\dot{M}$, the rate at which the hot gas cools below X-ray temperatures) are determined to be hundreds to thousands of solar masses per year. These rates depend on the X-ray luminosity within the cooling radius (the radius where the cooling time, t_{cool}, is equal to the Hubble time) and are calculated from the following equation:

$$\dot{M} = \frac{2\mu m L_{cool}}{5kT} \tag{1.1}$$

Here, T is the temperature of the hot gas, k is Boltzmann's constant, m is the mass of a proton and μ is the mean molecular weight of the elements in the hot gas. L_{cool} is the bolometric luminosity within the cooling radius. X-ray emitting gas at temperatures as low as only $0.3T_{virial}$ is measured (Fabian 2003). The virial temperature is the characteristic temperature of the gas and is found by equating the thermal and kinetic energies of a gas particle. For these clusters the virial temperature is typically 8keV (9.3×10^7 K).

O VI and many rotationally excited transitions of CO (such as CO J=(3-2) and CO J=(4-3)) have been seen which show that gases of respectively 100 000K and 20K exist (Edge 2003). Although the detection of Hα suggests the presence of hot stars, there is not enough Hα observed to account for the amount of matter deposited by the cooling flow (Voit 2003). Cooling flows are interesting as they may be an observable example of the ICM cooling to a low enough temperature to

allow star formation. However there have been many problems with the cooling flow scenario. Observational evidence for intermediate temperature X-ray gas (10^5-10^6K) would include the detection of the OVII and Fe XVII lines (Fabian et al. 2003), but so far these lines have not been detected. Also, until recently, there has been a lack of observed cool molecular gas as evidenced by molecular hydrogen emission at temperatures of 1000K.

Recent observations of the cool (1000K) and cold (20K) molecular gas in cooling flow clusters include Donahue et al.(2000), Jaffe et al.(2001), Edge et al.(2002) and Salomé & Combes (2003). The first group imaged the v=(1-0) [1] transitions of molecular hydrogen in the cD galaxies of three cooling flow clusters with the Near Infrared Camera and Multi-Object Spectrometer (NICMOS) on the Hubble Space Telescope (HST). Jaffe et al. (2001) and Edge et al.(2002) took K-band spectra of many cooling flow cluster galaxies and observed the v=(1-0) transitions of molecular hydrogen. Most recently Salomé & Combes (2003) mapped the cold CO (1-0) and (2-1) rotational transitions in the central cD of Abell 1795.

New higher resolution observations with the ASCA and Chandra telescopes have lowered the predicted mass deposition rates creating another problem for the classical cooling flow picture, the amount of molecular gas that is observed does not match the amount expected from a cooling flow. We observe more cool molecular gas than predicted.

As we now have observations of the high temperatures of the hot ICM, and we

[1] In this notation the v refers to a vibrational transition. The first number is the upper level and the second number is the lower level.

have detected cold molecular gas, the main problem with cooling flows can be summarized with the following question. Why is the X-ray gas not seen at intermediate temperatures if it indeed cools from the high temperatures of the ICM to the low temperatures of the molecular gas (Fabian 2003)?

Four possible solutions have been presented in the literature follow: (1) absorption, (2) inhomogeneous metallicity, (3) mixing and (4) heating. If absorption (1) occurs for only X-ray emitting gas below 3 keV (3.5×10^7 K) then the emission lines should not be able to be detected (Fabian et al. 2001). This is because the 3 keV gas is expected to be near the center of the cooling flow within the CDG, where the absorbing gas of the galaxy's interstellar medium exists. The inhomogeneous metallicity model (2) is attractive because the mass deposition rate expected from an inhomogeneous gas is much lower than that expected from a well mixed gas, and, for many clusters, is a better match to rates derived from high resolution X-ray data (Fabian, et al. 2001a). Mixing (3) of the predicted 10 000K gas with the hotter gas of the ICM could cause the intermediate temperature X-ray lines to become invisible (Fabian et al. 2001a). Mixing of the 10 000K gas with colder gas could also explain some of the optical emission lines seen in the centers of cooling flows. Although all the possibilities have some strong points, heating (4) is the most widely favored option as there are readily available sources. Heating can occur from outside the central galaxy, from an embedded active galactic nucleus (AGN), or from a combination of the two processes.

It is also important to note that strong magnetic fields can exist near the AGN in cooling flow clusters (CFCs) and that the coolest X-ray regions surround the radio

bubbles. These observational constraints must be preserved.

Almost all of the central galaxies in known CFC have an AGN. An observation which favors AGN heating is that the radio emission is seen to coincide with X-ray holes (regions in the ICM which are of low gas density and surrounded by bright rims (Fabian 2000)). One example is NGC1275, the CDG of Perseus as shown in Fabian (2000). Most cooling flow radio sources show this spatial anti-correlation to the X-ray emitting gas. It may not be a problem for heating models that all not every source shows the anti-correlation since radio sources vary on a shorter timescale than the X-ray emission. However, one problem with AGN models is that energies of about 10^{45-48} ergs/s are required from the radio source to heat the gas. It is difficult to achieve such a high luminosity; therefore, many favor a combination of AGN heating with another heating source, such as conduction within the hot gas (Tucker and Rostner 1983).

1.2.1 Motivation

CO and H_2 gas have been observed spectroscopically in the CDGs of many cooling flow clusters (Edge et al. 2002). Molecular gas is not seen in all central dominant galaxies (CDGs) of cooling flows. However, for every CFC for which cool molecular gas has been seen, there have also been positive detections of Hα emission (private communication, Edge 2003). A handful of central cD galaxies have also been imaged in Hα and in H_2 (Donahue et al. 2000). The morphologies of the atomic and molecular emission are always similar, although they do not correspond in detail (Donahue et al. 2000). Some CDGs that contain radio sources have been observed to

show structure in X-ray that is similar to the Hα. In the center of these clusters, the X-ray morphology seems to be anti-correlated with the position of the radio lobes. An interesting question is: What is the relationship between the different atomic and molecular emissions and why do their morphologies appear to correspond with each other?

Many other important questions are still unanswered concerning the cool gas (1000K) in cooling flow clusters. Jaffe and Bremner (1997) find that the inferred mass cooling rate from X-ray data is lower than the one inferred from H_2 emission at 1000K. Does there exist some heating mechanism that is warming a cooler more massive molecular cloud? What is the reheating mechanism that would raise the temperature of the molecular gas up to 1000K? Is it being reheated by shocks, UV radiation from hot stars or X-rays (Wilman et al. 2002)?

Of the three cooling flow clusters whose molecular hydrogen morphology has been observed, the emission is either extended or condensed. This morphology can give us clues to the questions asked above about the reheating mechanism. Perhaps extended and condensed emissions result from different physical processes, for example the condensed emission of some clusters could be due to an AGN and the more filamentary structure of others could be due to hot stars (Donahue et al. 2000).

The research presented in this thesis will attempt to address these questions by investigating the molecular hydrogen abundance and its morphology in Abell 1795. In Chapter two we use information gathered on properties such as mass deposition rate ($\dot{M}$), redshift and presence or absence of a CDG in order to pick this cluster.

We present the details of our observations of the image of Abell 1795 in the v=(1-0) S(1) [2] emission line of molecular hydrogen in Chapter 3. In Chapter 4, the image of molecular hydrogen in Abell 1795 is compared to images of Abell 1795 in other wavebands in order to determine to nature of the 1000K gas in this cluster and its reheating mechanism. Chapter 5 gives a summary of the results and conclusions.

[2]The capital s means the rotational transition goes from a lower level to an upper one and the number inside these brackets is the rotational quantum number of the lower level

Chapter 2

Determining the Sample

There exists no published up to date (lower $\dot{M}$ values) list of cooling flow clusters and their properties. Therefore, before any observations are planned a list of candidate cooling flow clusters must be gathered. Starting with 113 clusters collected from Peres et al.(1998), Fabian (1994), White (2000), Sodre et al. (2001) and Arnaud (1987)'s catalogues, Table 2.1 is formed. In picking out cooling flows from bright X-ray clusters it is necessary to choose only those that have a $\dot{M} > 0$ and a cooling time shorter than the Hubble time (10^{10} years). If a cluster has been specifically published as not having a cooling flow, for example some CFCs were found to be disrupted by a merger, then we remove it from the sample.

In generating our lists we also attempt to use only the newest values of $\dot{M}$ since data obtained with the newer ASCA and Chandra observatories imply lower $\dot{M}$. Therefore any $\dot{M}$ calculated using the data from these observatories (circa year 2000) are used. If only one value of $\dot{M}$ exists in the literature, and it was derived prior to the year 2000, the cluster is removed from the list. However, if two or more of these old values of $\dot{M}$ exist, than an average is used and the cluster is included. Appendix A shows the list of clusters from which our list of cooling flow clusters is formed.

2.0.2 Description of the Table

Our table of 36 CFCs is organized by $\dot{M}$ and contains seven columns.

The second column gives the cluster name, column three gives the cooling flow rate in units of solar masses per year, column four gives the cluster redshift and the fifth gives the Bautz-Morgan (BM) type [1] (if the BM type is unknown the field is left empty). The sixth column quantifies the degree of alignment between the optical emission peak of the CDG and the peak of the X-ray gas by listing their separation in arcseconds. We include these values in our table as they are based on data available to the public which we hope will give some insight as to which clusters may be interesting candidates for our observations. If there are no X-ray contours available the symbol "-" is used. An (E) is used to denote data from Einstein, an (R) for data from Rosat and a (C) for data from Chandra. If the cluster has two CDGs the distance is measured from the center of the X-ray contours to the midpoint of the two dominant cluster galaxies, and if the cluster has no dominant galaxies then the separation is measured from the X-ray peak to the nearest large galaxy. An offset of greater than one arcminute can be considered real (Drake 2002, private communication). The final two columns are the J2000 Right Ascension (RA) and Declination (DEC).

[1]The Bautz-Morgan type is a number that describes cluster morphology. Type I have a large centrally located cD, Type II have brightest galaxies which are intermediate between a cD and a normal elliptical and Type III have no dominant galaxies.

Table 2.1: List of Cooling Flow Clusters

	Cluster	$\dot{M}$ ($M_\odot$/yr)	Redshift	B-M	Separation (arcsec)	RA J2000	DEC J2000
1	A2204	916	0.1523	II	4(R)	16 32 45.0	05 34 42
2	PKS0745-191	702	0.1028		0(R)	07 47 30.9	-19 17 43
3	A478	570	0.0882		51(E)	04 13 25.0	10 27 59
4	A3112	430	0.0746	I	0(R)	03 17 57.7	-44 14 17
5	A2390	250	0.1237		44(E)	21 53 36.2	17 41 27
6	A1835	230	0.2523		0(R)	14 01 01.8	02 52 49
7	A644	214	0.0704	III	0(E)	08 17 25.5	-07 30 40
8	A2219	200	0.2281	III	0(R)	16 40 20.4	46 42 44
9	Cygnus-A	187	0.0570	I	0(R)	19 59 28.1	40 44 05
10	A1651	185	0.0845	I-II	29(R)	12 59 22.9	-04 11 09
11	A426	183	0.0183	II-III	0(E)	03 19 48.0	41 30 46
12	A1689	164	0.1810	I-II	9(E)	13 11 29.5	-01 20 28
13	MKW3s	151	0.0449		19(E)	15 21 51.8	07 42 24
14	A2199	150	0.0300	I	0(E)	16 28 37.7	39 33 03
15	2A0335+096	142	0.0349		18(R)	03 38 40.2	09 58 12
16	A2052	120	0.0348	I-II	13(E)	15 16 43.7	07 01 19
17	A85	108	0.0521	I	27(E)	00 41 50.8	-09 18 07
18	A1795	100	0.0627	I	5(C)	13 48 52.7	26 35 30
19	A2029	100	0.0767	I	0(E)	15 10 55.8	05 44 46
20	A496	98	0.0330	I	0(E)	04 33 37.6	-13 15 40
21	A3571	80	0.0391	I	6(R)	13 47 28.4	-32 51 55
22	Ophiuchus	75	0.0280		35(R)	17 12 27.8	-23 22 08
23	Klemola-44	71	0.0300	III	-	23 47 31.1	-28 12 10
24	A2142	69	0.0899	II	7(E)	15 58 20.2	27 1352
25	A2063	60	0.0350	II	1(E)	15 23 04.8	08 36 20
26	A2597	50	0.0824	III	18(E)	23 25 19.3	-12 07 20
27	A3558	50	0.0478	I	0(R)	13 27 56.5	-31 29 44
28	A262	47	0.0164	III	21(E)	01 52 45.4	36 09 26
29	AWM7	42	0.0172	I	14(E)	02 54 27.4	41 34 51
30	Hydra-A	29	0.0522		0(R)	09 18 05.8	-12 05 40
31	A4059	27	0.0478	I	0(R)	23 57 00.2	-34 45 39
32	A970	20	0.0587	III	52(E)	10 17 23.2	-10 41 09
33	Centaurus	18	0.0109	I-II	0(E)	12 48 48.9	-41 18 44
34	A400	10	0.0238	II-III	32(E)	02 57 37.4	06 00 45
35	A1060	9	0.0124	III	36(E)	10 36 43.2	-27 31 40
36	A576	6	0.0381	III	23(E)	07 21 31.2	55 45 52

2.1 Alignment of X-Ray and Optical Emission

We now have an extensive sample from which we can form an ideal target list. At this point we can use archived data and compare the X-ray contours to the optical images of these clusters. This will present us with additional information which we can use to select a target for molecular hydrogen observations.

The definition of a cooling flow cluster is based on a difference in the X-ray emitting gas properties in these clusters relative to other clusters. In cooling flow clusters the X-ray surface brightness shows a spike that is generally very close to the CDG which is located at the bottom of the gravitational potential well of the cluster. This is consistent with the picture of the CDG being connected in some way to the cooling flow.

However, the paper from Sodre et al.(2001) on the CFC Abell 970 presents an offset of 52" between the X-ray peak and the CDG. Even though for this cluster the misalignment is close to the pointing accuracy of Einstein, we conduct a rigorous archival survey of all publicly available cooling flow clusters. We ask how many, if any, cluster's optical and X-ray imaging data show a displacement between the CDG and X-ray peak. If we do find the two peaks are not aligned this is inconsistent with the picture of the CDG being affected by the cooling flow. However if the two peaks are aligned, a cooling flow origin of the molecular hydrogen we search for in Abell 1795 would be supported.

To find any offset between the optical center and the X-ray emission peak, the X-ray images available in the HEASARC public archives are displayed as contour

overlays on the Sloan Digital Sky Survey (DSS) images of the cluster (see Figures 2.1 to 2.6). STARLINK's GAIA reduction and analysis program was used to create the final image. For the X-ray contours we use Chandra data if it is publicly available, otherwise older ROSAT or Einstein IPC data is used. For clusters in Table 2.1 without public X-ray data we show only the DSS image.

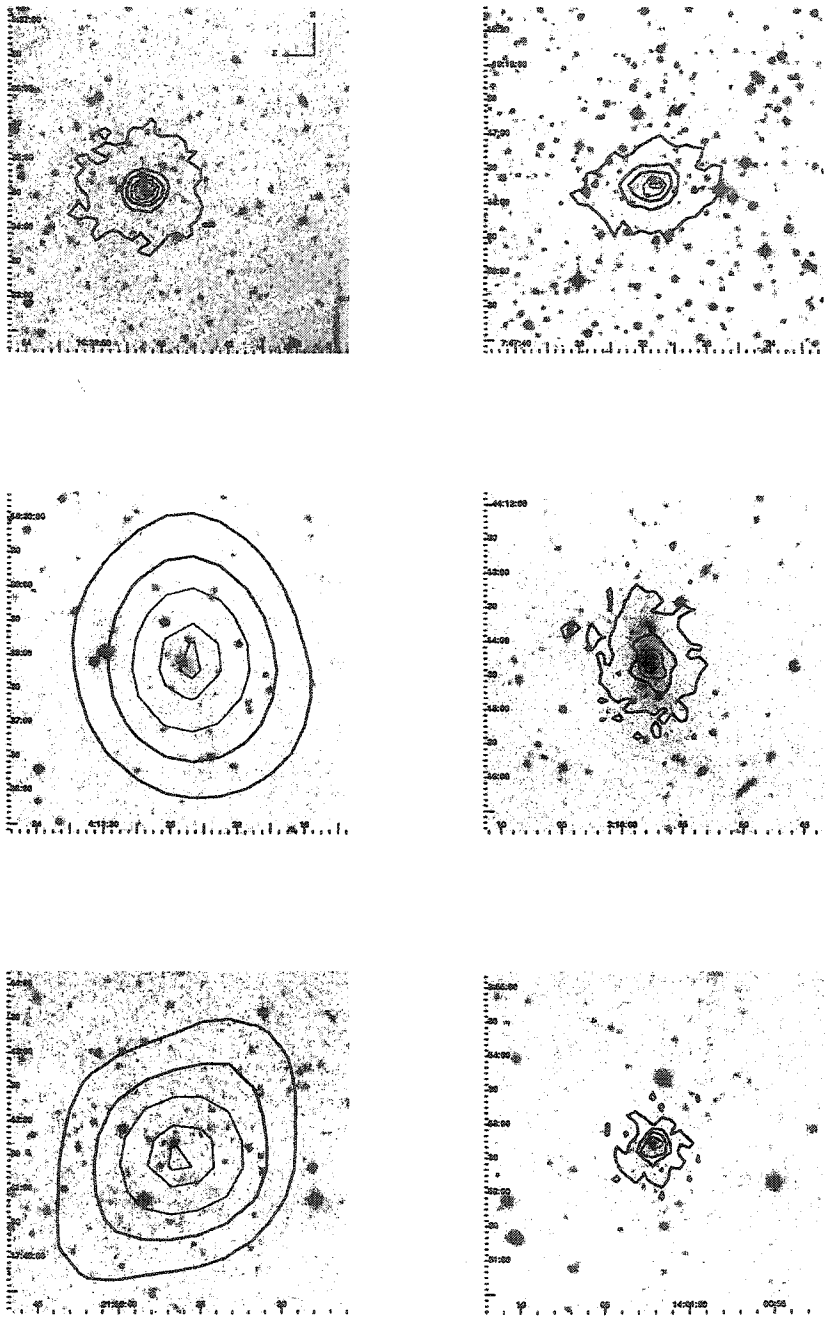

Figure 2.1: X-Ray contour images are superimposed on Digital Sky Survey images. X-ray data from the Rosat observatory is designated with an R, from the Einstein observatory is designated with an E and from the Chandra observatory is designated with a C. Clockwise from top left the clusters are: Abell 2204 (R), PKS 0745-191(R), Abell 3112(R), Abell 1835(R), Abell 2390 (E) and Abell 478 (E).

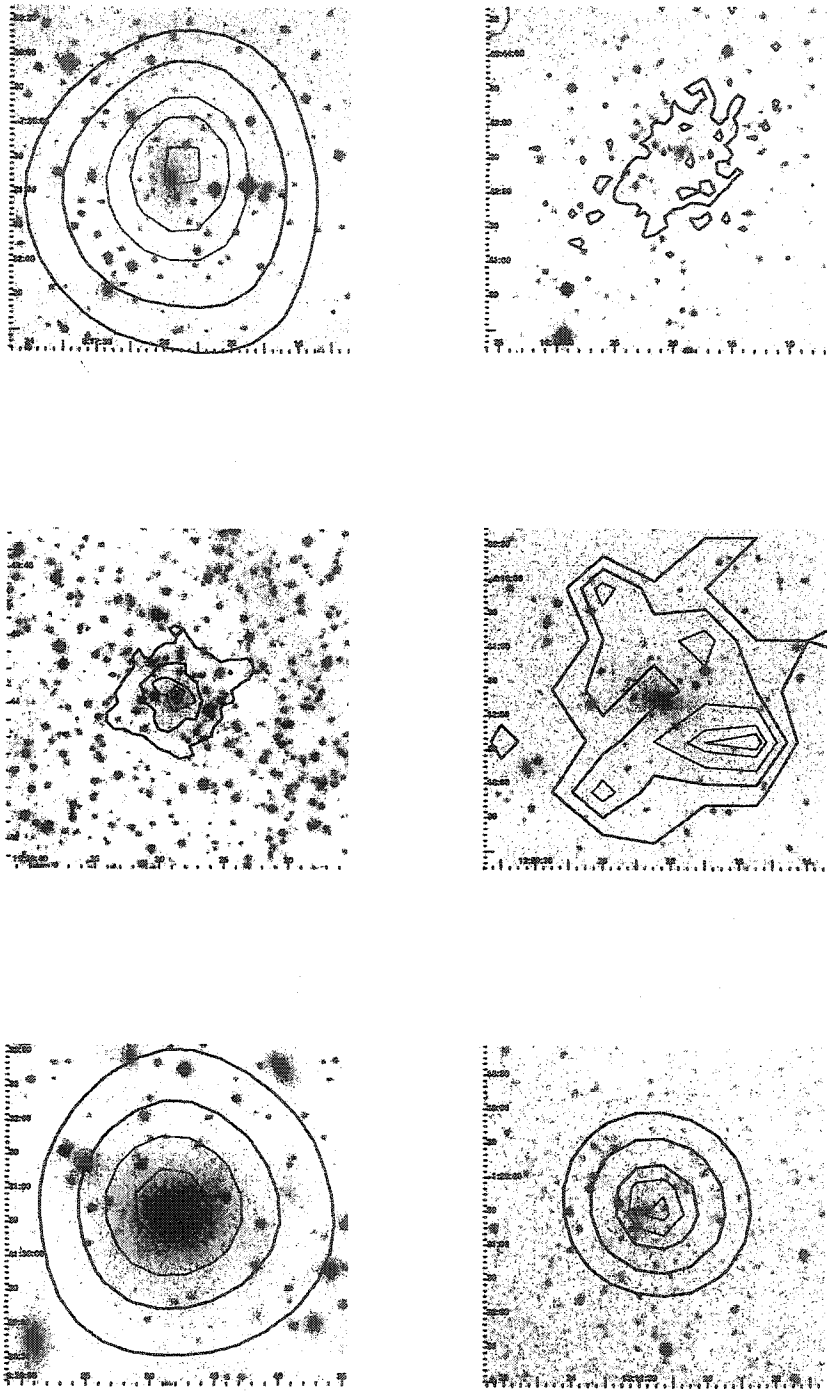

Figure 2.2: Continued from previous page. Clockwise from top left, the clusters are: Abell 644(E), Abell 2219(R), Abell 1651(R), Abell 1689(E), Abell 426(E) and Cygnus A(R).

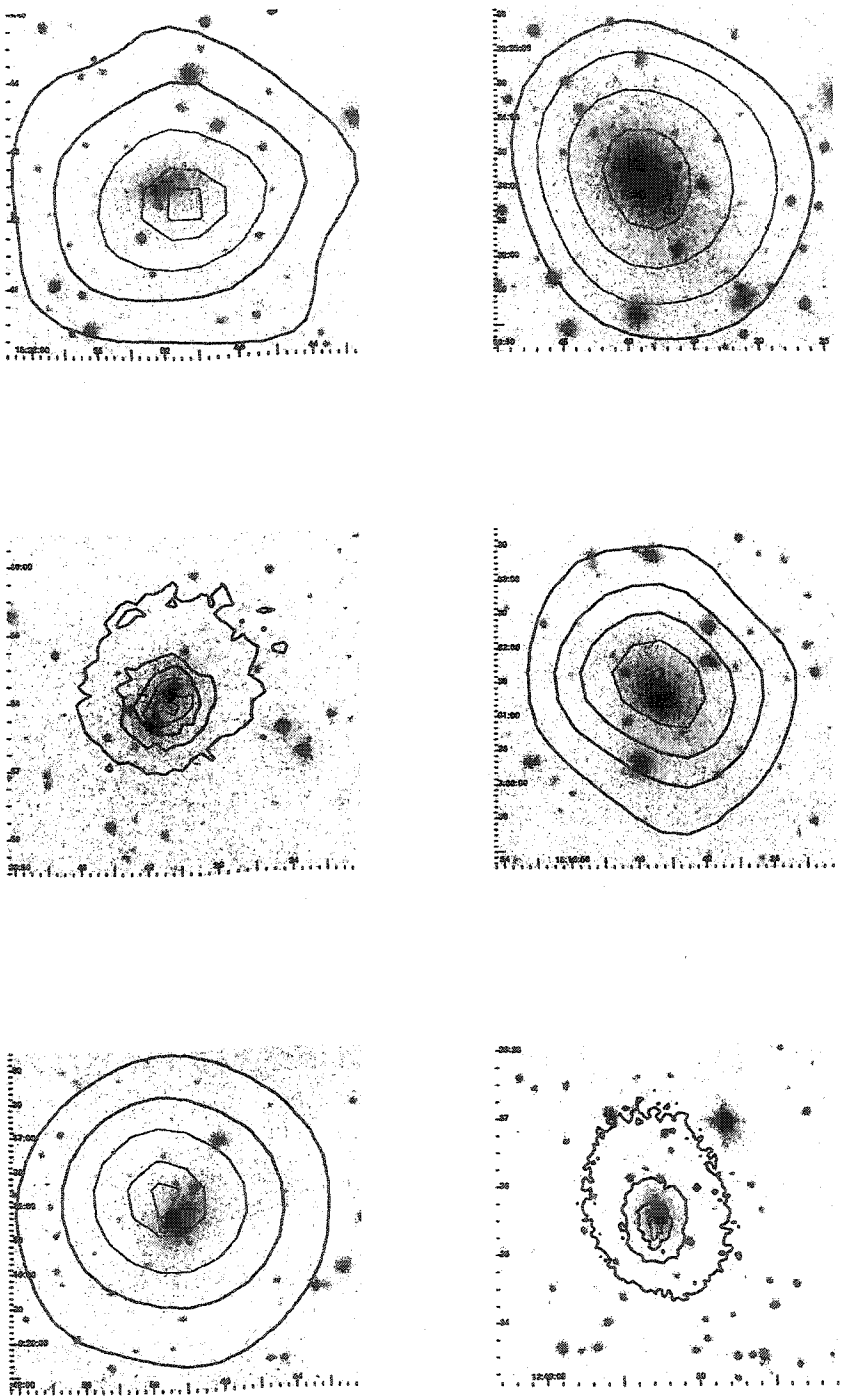

Figure 2.3: Continued from previous page. Clockwise from top left, the clusters are: MKW3 s(E), Abell 2199(E), Abell 2052(E), Abell 1795(C), Abell 85(E) and 2A 0335(R).

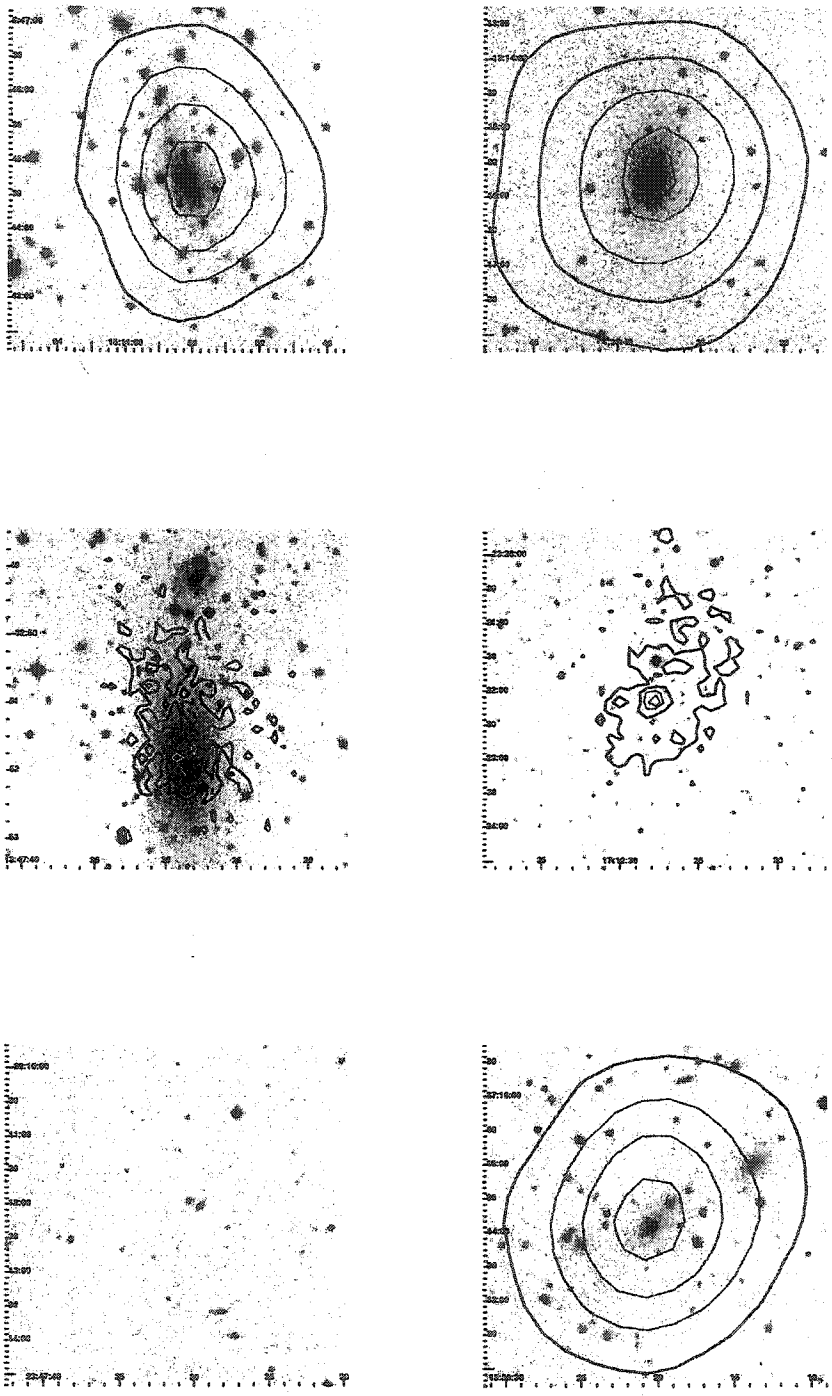

Figure 2.4: Continued from previous page. Clockwise from top left, the clusters are: Abell 2029(E), Abell 496(E), Ophiuchus(R), Abell 2142(E), Klemola 44, Abell 3571(R).

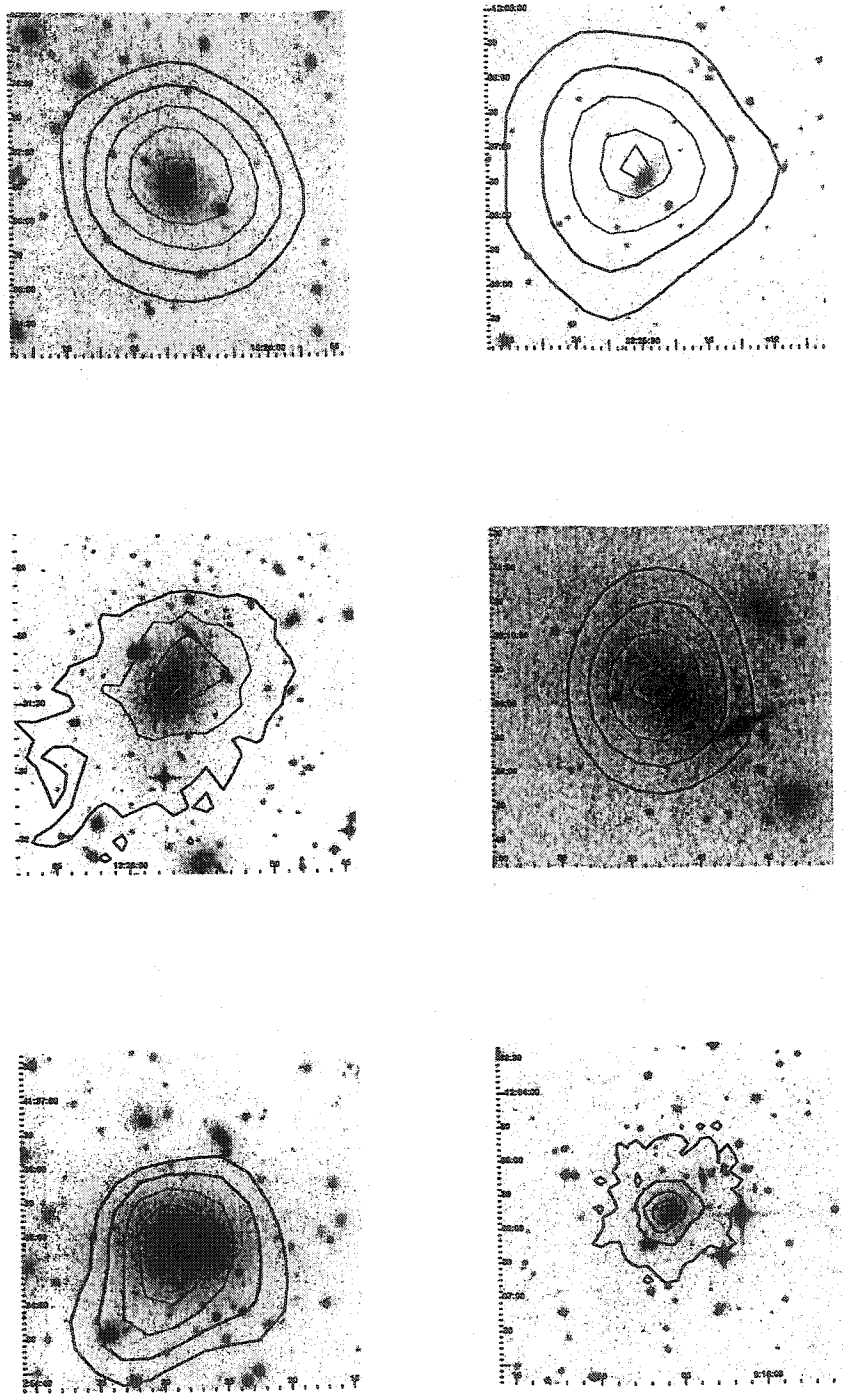

Figure 2.5: Continued from previous page. Clockwise from top left, the clusters are: Abell 2063(E), Abell 2597(E), Abell 262(E), Hydra-A(R), AWM 7(E) and Abell 3558(R).

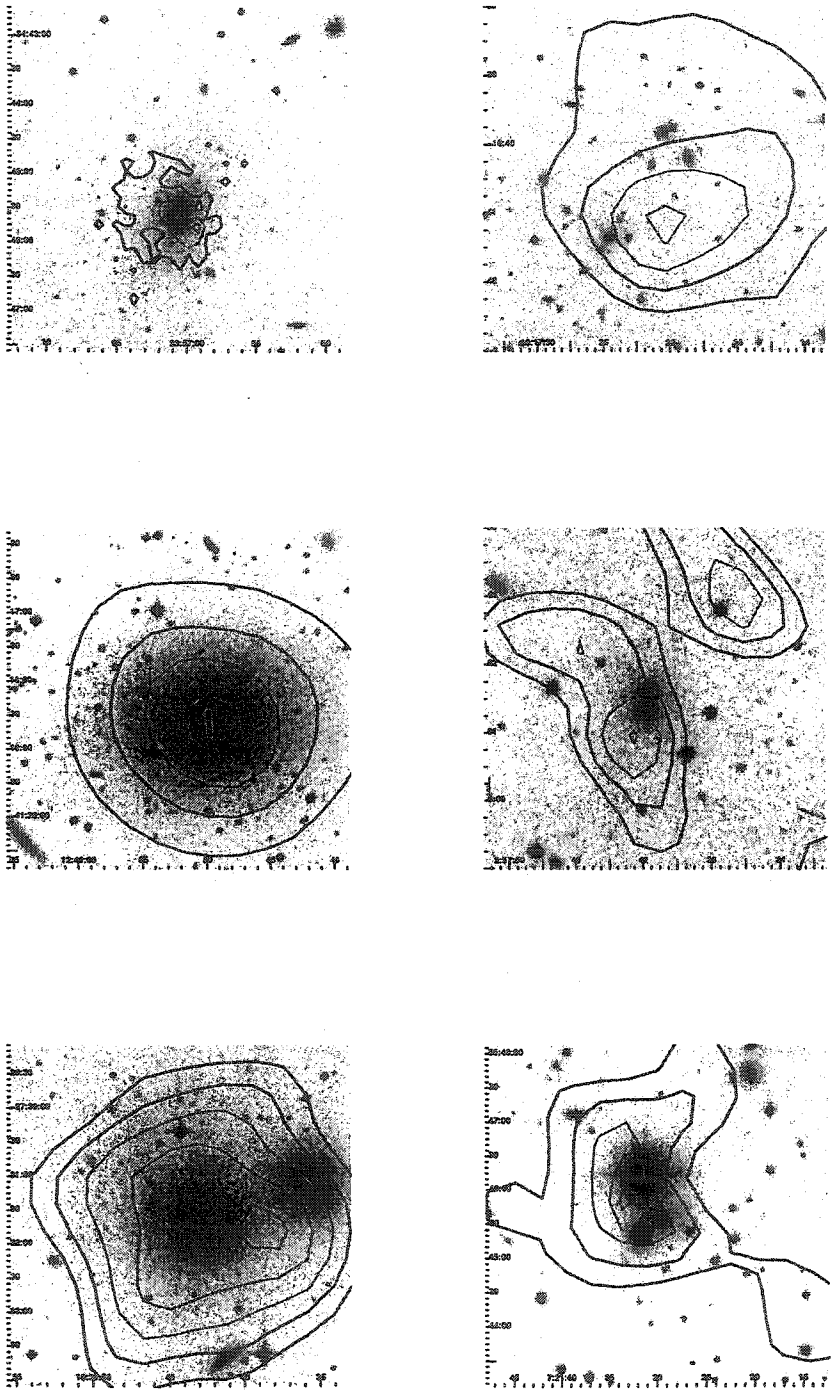

Figure 2.6: Continued from previous page. Clockwise from top left, the clusters are: Abell 4059(R), Abell 970(E), Abell 400(E), Abell 576(E), Abell 1060(E) and Centaurus(E).

2.2 Analysis of Cluster and X-Ray Properties

As shown in Figures 2.1 - 2.6 and Table 2.1, some of the clusters appear to have offsets of a few arcseconds up to just under an arcminute. We ask: How many of these are above the resolution and pointing accuracy of the telescope used for the measurements? Are the clusters of BM type II-III and III all at high redshift? And, is there anything interesting about clusters that have two CDGs?

There are 21 clusters with Einstein data, 13 with Rosat data and 1 with Chandra data. The resolution and pointing accuracy of the instruments on board the Einstein and Rosat observatories are such that separations under one arcminute cannot be considered real (Drake 2002, private communication). We have one cluster with X-ray data taken using Chandra. The instrument used on Chandra has a pointing accuracy of around 3 arcseconds as well as a resolution of 0.5 arcseconds. Therefore, the separation of the X-ray and optical emission peaks for Abell 1795 (5") can be considered real. This does not mean that the CDG was always displaced with respect to the peak of the X-ray emitting gas; this cluster in fact has a "tail" in the X-ray and the CDG has a peculiar radial velocity indicating that it is not at rest with respect to the gravitational potential (Fabian et al. 2001). It is thought that the CDG might oscillate through this pattern as it is pulled back and forth across the central gravitational potential of the cluster (Fabian et al. 2001). Thus, because of the morphology of the X-ray contours, it is not clear if the CDG was at some time aligned with the X-ray peak.

The Sloan Digital Sky Survey (SDSS) has a sensitivity of 23.1 in the R-band and

employs the same integration time on all fields. CDGs of clusters that are further away may not be detected simply because they are below the sensitivity limit of the SDSS. If this were a problem we were encountering then the distant clusters of BM type I-II may be mis-classified as type III. By examining the table however, it can be seen that all the clusters of BM type II-III or type III at a certain redshift are matched by clusters of BM type I or II at the same, or a higher redshift. For example, the BM type III cluster Abell 576 (entry 36) has the same redshift as the BM type I-II cluster Abell 2052 (entry 16). One exception is Abell 2219 which is of BM type III and has the highest redshift of known BM type clusters in our sample (z=0.2218). We calculate the magnitude of a typical cD galaxy at this redshift and compare with the sensitivity limit of the SDSS. Let us take the Coma cluster which has a z=0.085, or a distance of 345 Mpc (assuming everywhere that value of the Hubble constant is 71 km/s/Mpc), to be our typical cluster. The Coma cluster's CDG has a R magnitude of 15.74, which converts to an absolute magnitude of -22.13. If we then move this cluster out to the distance of Abell 2219, the magnitude becomes 17.9. This value is brighter than the sensitivity limit of the SDSS.

If the cooling flow adds stellar mass to the cD galaxy (Johnstone et al. 1989), we might expect the cooling flow clusters at high redshift, which represent a population of clusters at an earlier stage in their evolution, to have a less significant central galaxy. However, a sample of cooling flow clusters with a much larger redshift range would be required in order to show any statistically significant correlation that might exist.

An interesting case, Abell 400 has two CDGs and the X-ray peak is in the center

of these two. However, the separation is smaller than our error. Abell 478 and Abell 970 both have peak separations bordering on one arc minute.

This section has found only one cluster for which the misalignment is less than the positional accuracy. The misalignment of Abell 1795 however is only a few arcseconds, and the cD galaxy may be moving, therefore it is not clear, just from the alignment of the optical CDG and the peak of the X-ray emission, to what degree the CDG and cooling flow are related. There has been speculation that the cooling flow may have an effect on the evolution of the CDG by adding cool gas to these systems and perhaps even a young stellar population (Fabian 2003). There is also speculation that the X-ray tail is a cooling wake. In a cooling wake, gas with shorter cooling times drops out first, and gas with longer cooling times drops out further along the tail (Fabian et al. 2001). This idea is supported by observations of Hα and a UV excess, both signatures of recent star formation, for this cluster which occur in the same position as the X-ray tail (see Chapter 3, section 3.4, for more discussion). However, the X-ray gas must go through a cooler molecular cloud stage before star formation can take place, in order to remain consistent with the classical picture of cooling flows.

Recently it has been determined that central cluster galaxies that show optical line emission are closer to the cluster's X-ray peak than non-emitting galaxies (Crawford 2003). This finding, along with our result which shows the central cD galaxy of Abell 1795 not to be aligned with the peak of the X-ray gas, illustrate that there is not a simple answer as to whether the optical line emitting CDG may be a result of the cooling X-ray gas. One test we can perform is to image the cluster

in the v=(1-0) S(1) emission line of molecular hydrogen at 2.12 μm, which probes a lower temperature gas, to check if the cooling wake is found at this wavelength as well. Abell 1795 is the only one of our overlays for which the data was taken using Chandra (high positional accuracy) and it shows a separation in the optical and X-ray gas peaks. But its X-ray morphology is complex and in the next section we search for evidence of molecular gas, which may or may not originate from the cooling flow itself.

Chapter 3

Molecular Hydrogen in Abell 1795: Observations and Results

The rest of this thesis focuses specifically on the questions of where in the cluster Abell 1795 the H_2 and the optical emission are contained, and, if in fact the cooling flow modifies the central dominant galaxy. We first attempt to answer these questions by imaging, for the first time, the spatial distribution of the molecular hydrogen (H_2) near the center of the cluster.

In the very central regions of these flows, the gas is expected to become molecular. We expect H_2 emission from molecular gas at temperatures of order 1000K. Near-infrared spectra of galaxies associated with three CFCs were obtained by Falcke et al.(1998). They found that these CFCs are strong H_2 emitters. As mentioned in the introduction, Donahue et al.(2000) observed a sample of three CFCs (one of which is from the sample of Falcke et al.(1998)) with redshifts moving the H_2 v=1-0 emission line into the NICMOS filters. They also found H_2 emission.

In general, H_2 emission is found in regions that contain dust. Due to the hot temperatures of the ICM, dust is not expected to form or remain in this environment. Dust grains will not survive the hot temperatures of the ICM. But, as molecular hydrogen usually forms on dust grains, Donahue et al.(2000) conclude that the molecular hydrogen they observe did not form within the cooling ICM. On the

other hand, molecular hydrogen is not found in non-cooling flow clusters (Jaffe et al. 2001), and some authors suggest the H_2 is the cool material of CFCs.

The mass cooling rate from the H_2 line emission can be calculated using Equation 3.1 (Donahue et al. 2000) and is larger than the values derived from the measured X-ray luminosity (Equation 1.1, section 1.2).

$$\dot{M} = \frac{m_{H_2}\phi}{\eta} \tag{3.1}$$

In Equation 3.1, m_{H_2} is the mass of a hydrogen molecule, ϕ is the line luminosity in photons per second and η represents the amount of cooling expected from one H_2 v=1-0 emission line in IR (2-10 percent). The results from Equation 1.1 and Equation 3.1 differ by 2 orders of magnitude, with the larger values from Equation 3.1, suggesting the observed H_2 v=1-0 emission is not a product of the cooling flow. Searches for CO emission from the molecular gas have found only small amounts (e.g. Edge 2001, Braine and Dupraz 1994), suggesting that the cooling rate is much lower and highlighting the fact that the nature of cool and cold gas in CFCs is not well understood.

One explanation for the large $\dot{M}$ calculated from Equation 3.1 is that a large reservoir of cooler molecular gas is reheated by some mechanism, such as shocks, photo-ionization by an AGN (Bohringer et al. 2002) or a massive starburst in the central galaxy (Edge et al. 2001).

There remains confusion over the nature of the molecular gas and its heating mechanism in these objects. What is the excitation mechanism of the molecular

hydrogen? Shock heating would produce a large flux ratio of Hα/H_2 (greater than $\sim$30 for a shock with v > 50 km/s) as it is known that fast shocks dissociate H_2 molecules. For emission powered by UV photo-ionization from stars, a ratio of $\sim$3 is expected assuming the stellar UV sources that they are typical of those found in the Milky Way. Heating by an AGN would produce a ratio of $\sim$100, assuming a typical power-law spectrum for the AGN (Donahue et al. 2000). Donahue et al. (2000) find ratios of order 10 in their sample of 3 clusters, therefore they rule out heating by fast shocks and favor excitation by a young stellar population. However, there is no direct evidence to support this scenario, and the precise excitation mechanism is unclear. In addition, there are few detections of H_2 in the literature, so that there is little understanding of the systematic properties of H_2 emission in cooling flows. Do all cooling flows show H_2 emission? Does H_2 emission strength correlate with X-ray luminosity or optical emission lines such as Hα?

Edge et al.(2002) presented 32 CFCs with one or more of the H_2 v=1-0 emission lines observed spectroscopically in 23 of the systems. This group has also observed over 60 clusters in CO and detected 24 which contain rotationally excited CO.

The use of these spectra allows for observations of clusters that are now known to contain H_2. Clusters can be chosen which will then have both an observed spectral line of H_2 v=(1-0) S(1) at 2.12 μm and a near-IR image in the wavelength range including H_2.

There are at least three reasons why it is important to image the H_2 in CFCs that are already known to contain H_2. First, to check for spatial correlations of the H_2 and X-ray emission, second, to determine whether the emission is filamentary or

centrally condensed (as clues to the reheating mechanism), and third, as CFHT has a large field of view (3.6' by 3.6'), these observations should reveal any emission in surrounding galaxies if it is present.

3.1 The Proposed Observations

We put in a proposal for CFHT (principal investigator Louise Edwards, see Appendix B) that was granted 3 nights using CFHT-IR in mid December, 2002 to observe H_2 in 3 CFCs. Unfortunately, the filter wheel for CFHT-IR was stuck for the three nights so that observations using this instrument were also impossible.

Appendix B also shows a Gemini proposal (co-investigator Louise Edwards) for which we were awarded time to do spectroscopy on a sample of CFCs using Flamingos I. However, the instrument on Gemini broke and we were not able to collect our data.

To make up for our lost nights in December, we were given one night of engineering time with CFHT-IR in April 2003. We decided to use this one night to observe H_2 in one CFC as in our original proposal to CFHT. In order to choose a good candidate for our one night, we followed the same procedure in picking the original December targets.

Our target was selected based on the following criteria: 1) a spectroscopic detection of the H_2 v=(1-0) S(1) line exists, 2) detections of CO or Hα are available 3) the redshifted H_2 v=1-0 S(1) line falls in one of the available filters 4) the target is visible for a long enough period in mid-April, 2003 to be detected at a signal to

noise of 5 (see section 3.1.3).

In terms of visibility, a full moon is not considered a problem since the observations are in the infrared and the moonlight as well as twilight is mostly scattered to short wavelengths. On the other hand, a large airmass may represent a huge problem as water vapor causes extreme extinction at infrared wavelengths thus we did not observe a target at an airmass larger than 1.5.

We selected Abell 1795 because it is visible for a total of 6 hours, is one of the CFCs for which H_2 v=(1-0) S(1) is detected spectroscopically (Edge 2002) and can be detected with only one night of observations (see section 3.1.3). This cluster has been extensively studied in radio, X-ray and optical (Fabian et al. 2001a, Pinkney et al. 1996), and from our study in Chapter 2 we know its X-ray morphology is complex. This cluster has never been imaged in H_2, and such observations only exist for 3 other clusters.

3.1.1 The Cluster Abell 1795

Abell 1795 is a rich cluster of BM type I which indicates that it has a single CDG. According to the Chandra X-ray observations of this cluster, the peak of the X-ray emission is a few arcseconds west of the cD galaxy and is extended to the south (see Figure 4.1, section 3.4). Most of the X-ray emission does lie near the central galaxy. Recall that the X-ray tail may be a wake caused by the oscillation of the cD around the cluster potential (Fabian et al. 2001b).

In addition to the IR and UV spectra, images of the cluster's cD galaxy have been taken in radio, X-ray, Hα, U-band as well as many optical images with HST

(F160N, F196N, F702W, F555W, F200N and F814N). The flux of the H_2 v=(1-0) S(1) emission line has already been determined from the spectral observations of Edge et al.(2002) and Jaffe and Bremer (1997). An Hα flux has also been determined (McNamara et al. 1996). This CFC has been extensively studied.

Current data on Abell 1795 show significant evidence of recent star formation in this CDG: Hα emission is detected in the cD and a UV excess is also measured. The X-ray emission, Hα emission and U-band data all show similar "tail" structures.

This cluster's CDG morphology in H_2 could be very interesting. We know that H_2 exists, but does it exhibit the same large scale morphology as that seen in Hα, X-rays and U-band?

3.1.2 Technical Considerations

Abell 1795 has a redshift of 0.0627 and thus the v=(1-0) S(1) transition of H_2 which is at a rest wavelength of 2.12 μm is expected to shift into the K Continuum (KC) filter available with CFHT-IR. The KC filter has a central wavelength of 2.26 μm a bandwidth of 0.06 μm (Figure 3.1, left). Edge et al.(2002) have published a spectrum in this region and they show that the H_2 v=(1-0) S(1) emission line is present. Their spectrum is shown in Figure 3.2.

The CO filter is used to measure the continuum only (Figure 3.1, right). The coverage is 2.29-2.31 μm.

The continuum image (CO) is subtracted from the image that contains the continuum and the H_2 v=(1-0) S(1) line (KC). The full width half maximum (FWHM) of the KC filter is 0.06 μm and that for CO is 0.02 μm, a factor of 3 smaller. There-

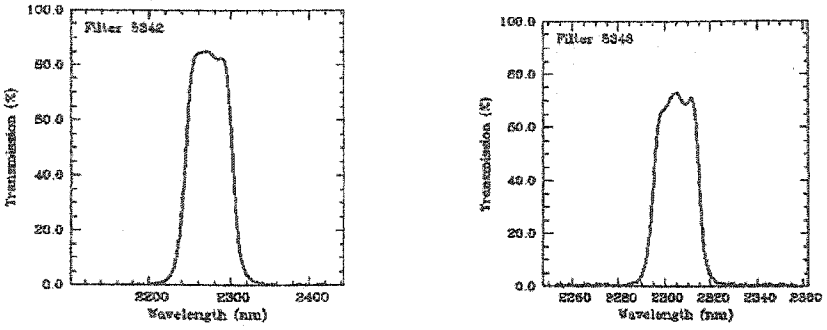

Figure 3.1: Transmission curves of the KC (left) and CO (right) filters. These figures are taken from the CFHT-IR website.

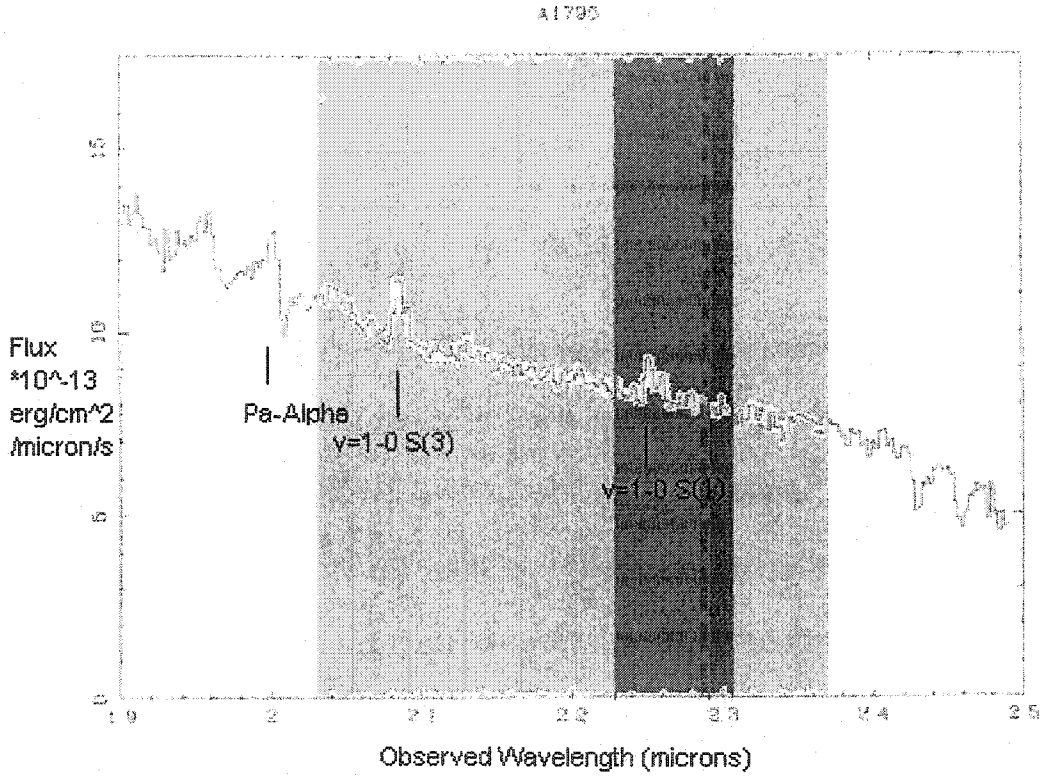

Figure 3.2: The K-band spectrum (solid line). The K-band is light grey, the pass band of the KC filter is medium gray and the CO filter is dark gray. The dashed region indicates the overlap between the KC and CO filters. Notice the v=(1-0) S(1) molecular hydrogen line falls inside the KC filter and the CO filter contains only continuum emission. This figure has been modified from Edge et al.(2002).

fore to obtain the same number of photons in each filter we integrate for 3 times as long on the source in the CO filter.

3.1.3 Estimate of Integration Time

To estimate the integration time required to detect the H_2 at the 5σ level, we use the line flux measured by Jaffe and Bremer (1997), 1.58×10^{-18} W/m^2.

We estimate an area of 3.14 "^{2} for the H_2 emission by measuring the area of H_2 emission in the CFC Abell 2597 observed by Donahue et al.(2000) which has a redshift similar to Abell 1795. Given a filter width of 0.06 μm for the KC filter and an area of 3.14 "^{2} for the spatial extent of the galaxy, we calculate a flux per μm per "^{2} of 8.38×10^{-18} W/m^2/μm/"^{2}.

We then estimate the contribution from continuum emission. There is no listed K-band magnitude of Abell 1795; therefore, we use the magnitude for the CDG of Cygnus A which is also a CFC CDG at a similar redshift. The K-band magnitude of the CDG of Cygnus A is 12.68 in an aperture of radius 5.76" (Lebofsky 1981) and the K-band flux per μm for a zero magnitude star is 4.07×10^{-10} W/m^2/μm. Therefore we calculate the mean surface brightness of the galaxy within the 5.76" radius aperture to be 3.32×10^{-17} W/m^2/μm/"^{2}.

The CFHT-IR webpage advertises a sensitivity of 20.1 magnitudes per "^{2} in the K filter for an extended source with 1000s integration time for a 5 σ detection. This magnitude is transformed into a flux and multiplied by the flux of a zero magnitude star to obtain a sensitivity limit of 3.71×10^{-18} W/m^2/μm/"^{2}.

To find the integration time needed for a detection with a signal to noise (S/N)

of 5 we use Equation 3.2

$$S/N = Cr_o t^{1/2}/(r_o + 2r_c)^{1/2} \tag{3.2}$$

where C is a constant, t is the integration time, r_o is the line flux per μm per $"^2$ and r_c is the continuum flux per μm per $"^2$. The constant C is determined by taking the brightness of the galaxy continuum to be zero giving Equation 3.3

$$S/N = Cr_o^{1/2} t^{1/2} \tag{3.3}$$

Using a value of 1000s for t, 5 for S/N and 3.71×10^{-18} W/m^2/μm/$"^2$ for r_o, we obtain 8.2×10^7 for the value of C.

We now solve for the integration time need to achieve a 5σ detection:

$$t^{1/2} = \frac{5(r_o + 2r_c)^{1/2}}{8.2 \times 10^7 r_o} \tag{3.4}$$

and find an exposure time of 1.1 hours is required in the KC filter. To measure the continuum in CO with the same signal to noise ratio, we need 3×1.1 hours or 3.3 hours.

3.2 Observations

A copy of the observation log is given in Appendix C.

Dark frames are taken in order to subtract the electronic offsets and extra photon flux due to the emission from the telescope and camera.

Dome flats are taken in each filter with the light on and off. Flat fielding removes pixel to pixel sensitivity variations. If the value of the flat with lights off is subtracted from the value of the flat with the lights on, a more accurate flat field is obtained as any hot spots or any thermal emission will be removed.

The CCD saturates at ~35 000 counts on the order of a few minutes therefore we were careful to keep the integration times low enough not to saturate the CCD. Thus, data cubes are formed of many short integration frames. A five point dither pattern is also used for cosmic ray rejection.

The standard star, FS18 is observed in KC for 600s and in CO for 1140s in order to flux calibrate our target. Abell 1795 is observed with a total integration time of 5116s in KC and 14040s in CO. This is a factor of 2.7 longer in CO, almost the factor of 3 we require. A set of frames consists of five dither positions, with an integration time of 360s per dither position in the CO filter and 246s in the KC filter. According to our integration time estimates we should obtain a 5σ signal since we have a total of 1.4 hours and our estimate is 1.1 hours (see section 3.1.3).

3.3 Data Reduction

To create sky subtracted frames we use the IRAF package DIMSUM (Deep Infrared Mosaicing Software, UM..., Stanford et al. 1995).

First the flat field frames are combined and the "light-off" combined frame is

subtracted from the "light-on" combined frame. The resulting flat is used to create a bad pixel mask. By plotting a histogram of the normalized flat field one finds many bad pixels above on the low and high ends of the histogram. These are flagged in order to create the bad pixel mask. Before running the first pass of DIMSUM, all the raw frames are flat fielded.

IR frames are completely dominated by sky emission, so it is essential to remove the sky. DIMSUM achieves a good sky subtraction by running two passes.

The first pass, creates a sky image from the two frames nearest in time to the frame to be sky-subtracted. Pixels with extremely low or high values are rejected and the remainder of the pixel values are averaged to form the sky image. The bad pixels are identified using the mask and are replaced by the value of their nearest neighbors.

After DIMSUM's first pass the width of each pixel is reduced by a factor of two, the image shifts are calculated interactively and the cosmic ray hits are removed. The final step is the mask pass which repeats the above steps to a high accuracy and combines the frames. The pixel values in the final frame have units of counts per second (DN/s).

3.3.1 Flux Calibration

We use the standard star FS18 to calibrate the flux of our target. First we find the magnitude of the star in each of the filters, then we find the zero point before applying it to the target.

FS18 has a K-band magnitude of 10.537 listed on the Joint Astronomy Center

webpage. Both the KC and CO filter passbands lie within the wavelength range of the K passband. In order to find the magnitude of FS18 in the KC and CO filters, we assume the flux per μm is constant over the entire K-band and multiply by the bandwidth of the two filters. The K-band is 0.336 μm wide and we calculate the magnitude of FS18 to be 13.59 in CO and 12.40 in KC.

To solve for the zero point Equation 3.5 is used

$$m_{ZP} = m_{ss} + 2.5 \times log(DN/sec) \tag{3.5}$$

where m_{ZP} is the zero point magnitude and m_{ss} is the magnitude of the standard star. For KC, the zero point magnitude is 22.69 and for CO it is 22.63. The zero points of the two filters are the same for practical purposes and we use a value of 22.6 in Equation 3.6.

Now the m_{ZP} can be applied to flux calibrate our CO and KC images. The transformation is done using Equation 3.6 for Abell 1795

$$m = m_{ZP} - 2.5 \times log(DN/sec) \tag{3.6}$$

3.3.2 Continuum Subtraction

We now need to subtract the continuum to get only the H_2 emission.

However, before subtracting the CO frame from the KC frame, we perform three additional steps. First, the images are aligned using the IRAF task IMSHIFT. The

alignment is accurate to 0.5 pixels as we subpixelated before the second pass of DIMSUM. The second step is to match the point spread functions (PSF) of the images in the two filters. This was done with the IRAF task PSFMATCH which smears out the smaller PSF of the KC filter, to match the PSF of the CO filter. Third, another correction between the two filters is applied, as they have different transmission efficiencies and we did not integrate on CO a full factor of 3 longer. To find this calibration factor we apply a simple test. As stars should not contain molecular hydrogen, we scale the CO to KC standard star frames so that the star disappears when the CO image is subtracted from the KC image. We then use this calibration method for the target frames. Flux in stars left over in the target frames (for example, Feature *d* in Figure 3.5) define our error of the continuum subtraction process. The remaining emission in the CDG, taking into account our error, is attributed to the H_2 v=(1-0) S(1) emission line. The image of the H_2 + continuum taken in the KC filter is shown in Figure 3.3, the image of continuum only taken in the CO filter is shown in Figure 3.4 and the final subtracted image of only H_2 is found in Figure 3.5.

We use aperture photometry with the image reduction program GAIA to measure the total count for the residual image of the CDG. The counts within successively larger aperture radii are summed and recorded on a graph of counts versus aperture radius. The total count is then measured within the aperture at which the curve of counts versus aperture radius reaches a plateau. The curve reaches a plateau at an aperture radius of about 15 arcseconds from the center of the CDG. In order to insure that excess counts due to emission from the surrounding galaxies does not

pollute the measurements for the CDG, pixel values for nearby galaxies are replaced by an average value of the background.

The magnitude of the H_2 emission from the CDG as seen in Figure 3.6 and as Feature *a* in Figure 3.5 is 19.62, which corresponds to a total flux of 1.93 +/- 0.79×10^{-18} W/m^2. As mentioned previously in this section, our error is derived from the flux left in the star (Feature *d* in Figure 3.5) and is due to errors in PSF matching and alignment. From spectroscopy, Jaffe et al. (2001) find an H_2 emission flux of 1.58 +/- 0.1×10^{-18} W/m^2 and Edge et al.(2002) find 5.9 +/- 2.1×10^{-19} W/m^2 in the CDG of Abell 1795. Our results confirm those of Jaffe et al. (2001) to within experimental uncertainty. Also, since we now have an image of the continuum emission in the K-band, we can verify our estimates of integration time. Previously we had assumed a continuum emission that was the same as that of Cygnus A. Using the values that we now have for Abell 1795's continuum flux (4.8×10^{-17} W/m^2 from Figure 3.2) within a 2.6" aperture radius (from our own observations in the CO filter), and repeating the steps listed in section 3.1.3, an integration time of 1.23 hours is required for a 5σ detection. This number is in agreement with the estimate derived in section 3.1.3.

Features *b*, *c* and *f-i* are interesting as emission in these surrounding galaxies is unexpected. This will be discussed more in section 4.5. Feature *e* of Figures 3.4 and 3.5 is an instrumental artifact and should be ignored. It was present in only the second frame of each set of 5 dither positions. There are two factors which contribute to the non-smooth appearance of the final frames. First of all, because the final image is composed of a mosaic of frames centered on different positions, some

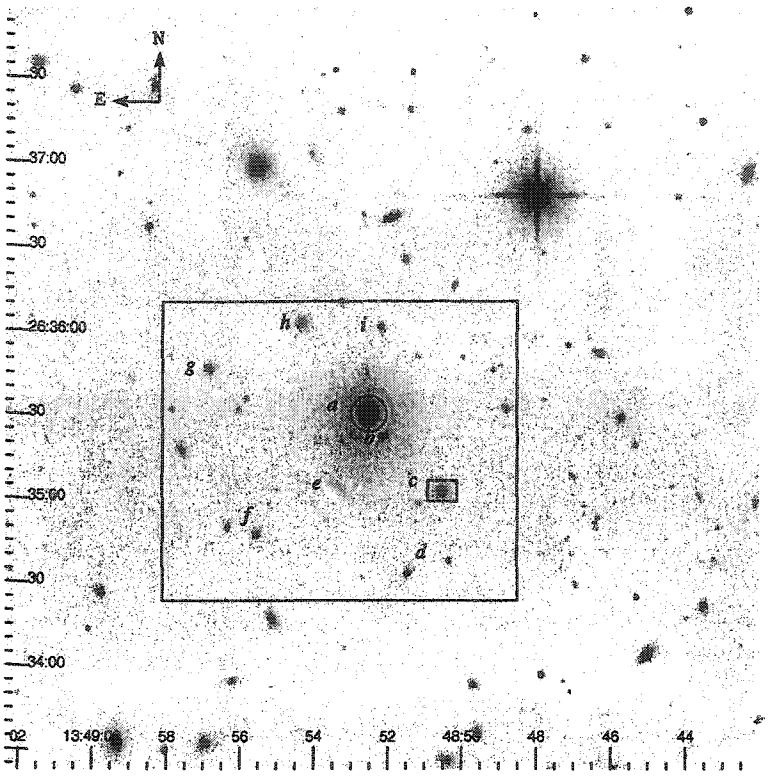

Figure 3.3: A 4.5' by 4.5' field of view of the image of A1795 using the KC filter (H_2 plus continuum) is shown. This image shows Features *a*-*i* (as discussed in the text). A circle is placed around the CDG and a rectangle around Feature *c*. In this image dark features represent emission.

areas have a higher signal to noise ratio than others. Second, faint horizontal streaks can be noticed throughout the images and are a product of the "reset anomaly," which occurs during the readout of the CCD.

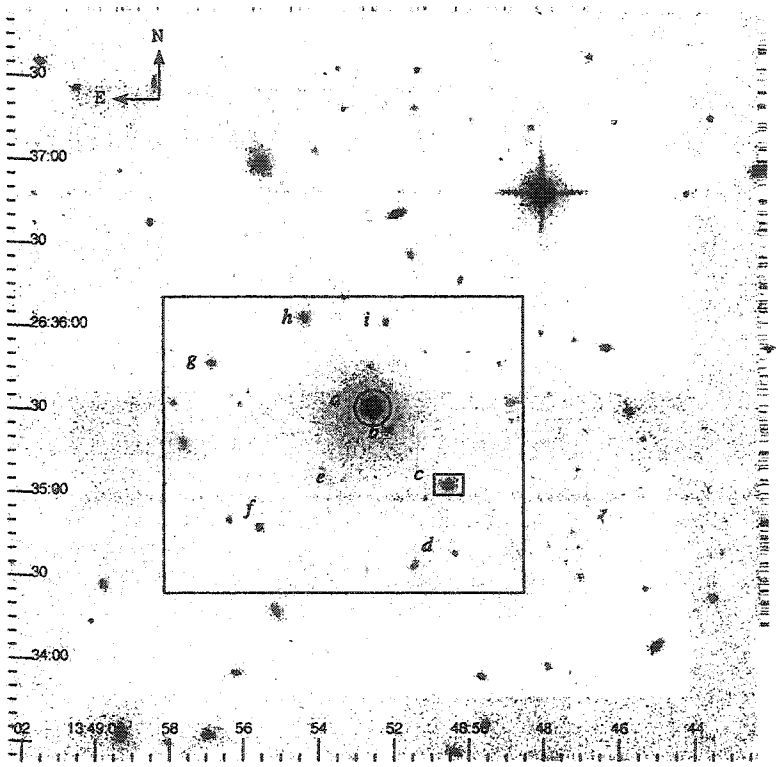

Figure 3.4: A 4.5' by 4.5' field of view of the image of A1795 using the CO filter (continuum only) is shown. This image shows features *a*-*i* (as discussed in the text). A circle is placed around the CDG and a rectangle around Feature *c*. In this image dark features represent emission.

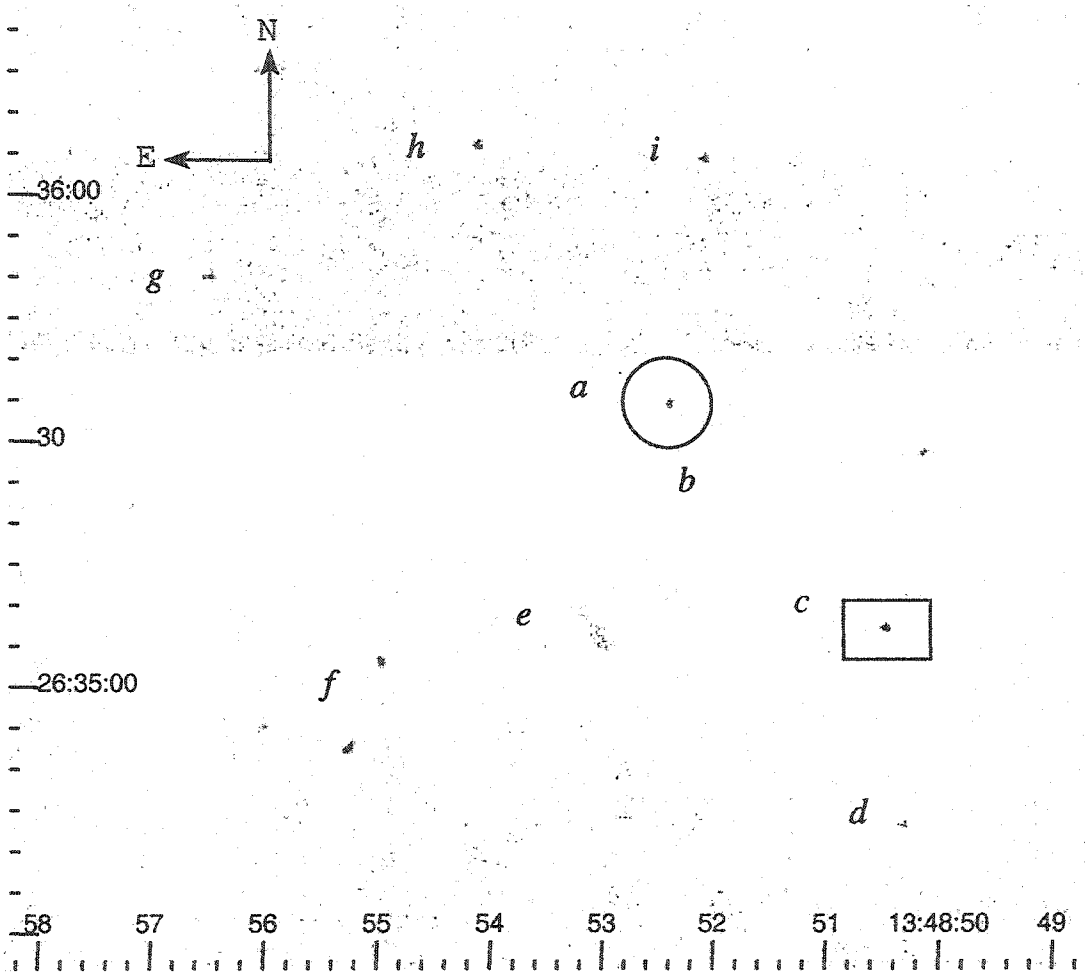

Figure 3.5: A 2.0' by 2.0' field of view of the image of H_2 emission in Abell 1795 is shown. This region corresponds to the area inside of the large rectangle in Figures 3.3 and 3.4. A circle is placed around the CDG and a rectangle around Feature *c*. In this image dark features represent emission.

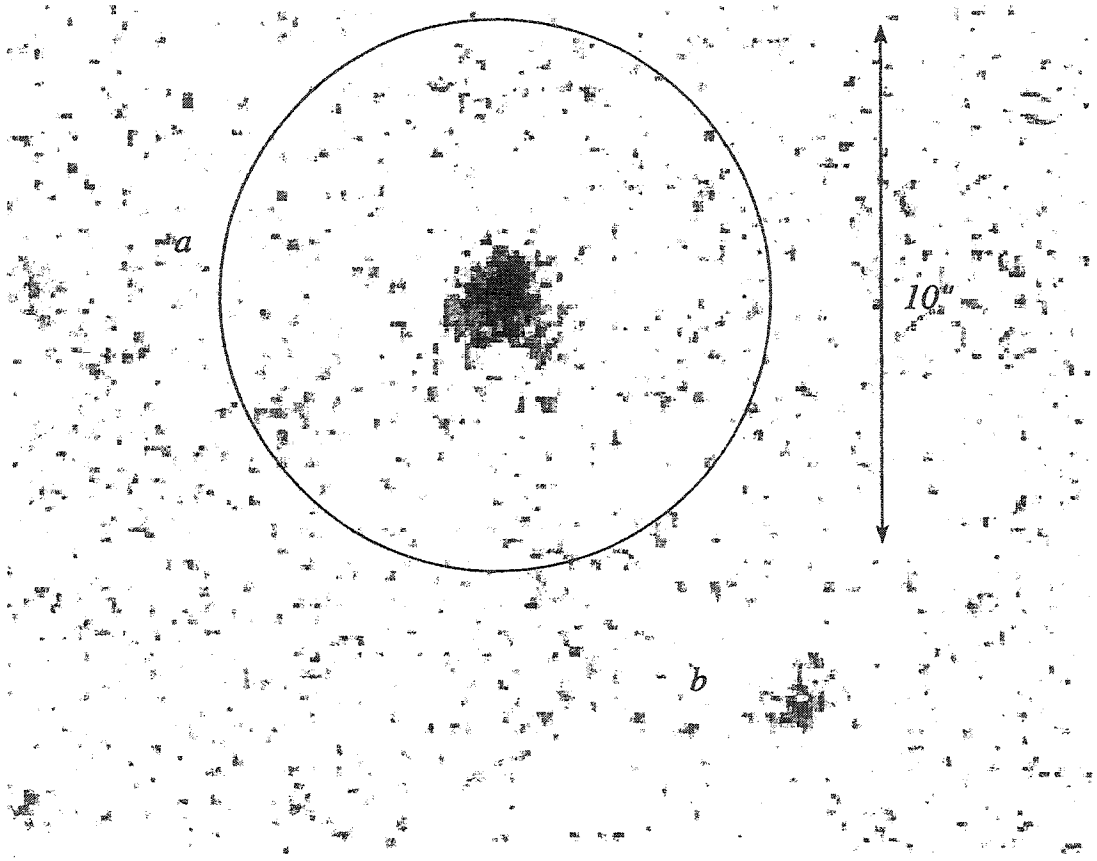

Figure 3.6: An image the H_2 emission in the CDG of Abell 1795. This close-up shows the condensed nature of the H_2 emission in the CDG. Dark features represent emission.

Chapter 4

Molecular Hydrogen in Abell 1795: Analysis

In this chapter we relate the molecular hydrogen images to those of the cluster at other wavelengths. This way, we can compare the H_2 morphology with that of tracers of recent star formation and determine the emission mechanism of the molecular hydrogen.

There is some evidence that the X-ray emitting gas is generally related to Hα emission, an optical emission line known to trace recent star formation. For example, it is known that close to a third of all CDG have optical Hα emission. The center of a CDG which shows Hα emission is typically closer to the peak of the X-ray emission than it is when the CDG shows no Hα emission (Crawford, 2003).

Emission from H_2 is known to exist only when Hα emission is present (private communication, Edge 2003). Is there a close relationship between the H_2, the Hα and X-ray emitting gas? In the classical picture of cooling flows, the X-ray emission defines the cooling flow, the Hα emission is a tracer of star formation, and the H_2 comes from cool gas. Therefore, H_2 detections spatially correlated with Hα and X-ray emitting gas would serve as evidence for a connection between star formation, the cool gas reservoir, and the cooling flow. Recently images of cool molecular gas, CO J=(1-0) and J=(2-1) in Abell 1795 have been analyzed (Salomé & Combes

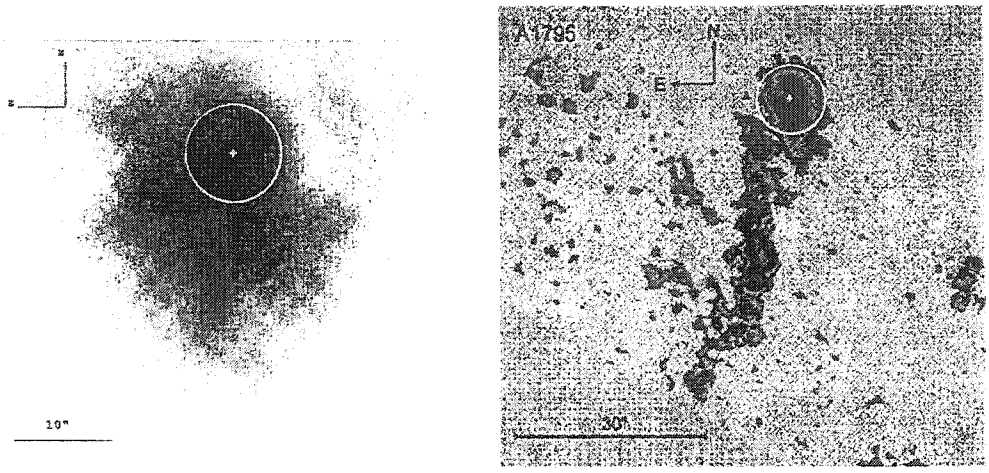

Figure 4.1: Images of X-ray gas on the left (1.0' by 1.25') and $H\alpha$+[NII] emission on the right (same scale as X-ray image). These images show the large scale similarities in the structure of the the X-ray and Hα emission features. Dark shades represent strong emission and the position of the CDG is marked with the symbol '+'. The extent of the CDG in the optical is shown as a light gray circle (radius = 5"). Adapted from Fabian et al. (2001a) and from Cowie (1983), respectively.

2003). The images show that the maximum brightness of the CO emission is located at the same position as the maximum brightness of X-ray and Hα emission. Is the maximum brightness of the H_2 emission in the same region as the CO, X-ray and Hα emission? And does emission at these wavelengths in turn correlate with the signature of young hot stars, UV excess? Like many other CFCs, Abell 1795 hosts an AGN, could the strong radio source at the center of the CDG have an effect on star formation?

4.1 Hα and X-ray

The same tail-like feature appears in the Hα emission and the X-ray emission (Figure 4.1). It extends about 80kpc (at the redshift of Abell 1795 1kpc = 0.6") directly

south of the peak emission (Crawford 2003). To answer our question above about the location of the Hα emitting gas, the molecular hydrogen emission is presented on the Hα image in Figure 4.2. Although Hα and H_2 emission are present in the CDG (the region inside the circle), as well as in Feature *c* (the region inside the rectangle) all of the emission features do not correspond (Figure 4.2). The peak of the H_2 and Hα emission match, however, the tail structure is not apparent in the H_2 image. We find that the H_2 emission is behaving like the Hα emission, although a deeper image of Abell 1795 is required to detect faint emission in the region of the tail, if it exists.

The X-ray emission is also shown as contours on the molecular hydrogen in Figure 4.3. This figure also illustrates what we learned from the image of Hα emission, that the H_2 emission does not show a tail. Note that the center of the H_2 emission is perfectly aligned with the peak of the Hα emission, yet displaced from of the peak of the X-ray emission. This advances the notion that the H_2 emission does not follow the X-ray emission.

4.2 U-Band

The U-band has a bandwidth of 680 Å and is centered at 3650 Å capturing the UV light. At a redshift of 0.06, the U-band covers 3549 to 4229 Å and contains mostly continuum emission. However, the O[II] (λ_{rest} 3727 Å) emission line falls within the U-band filter. McNamara et al.(1996) subtract a smooth profile from an HST U-band image of Abell 1795 and find many residual features. This is the UV

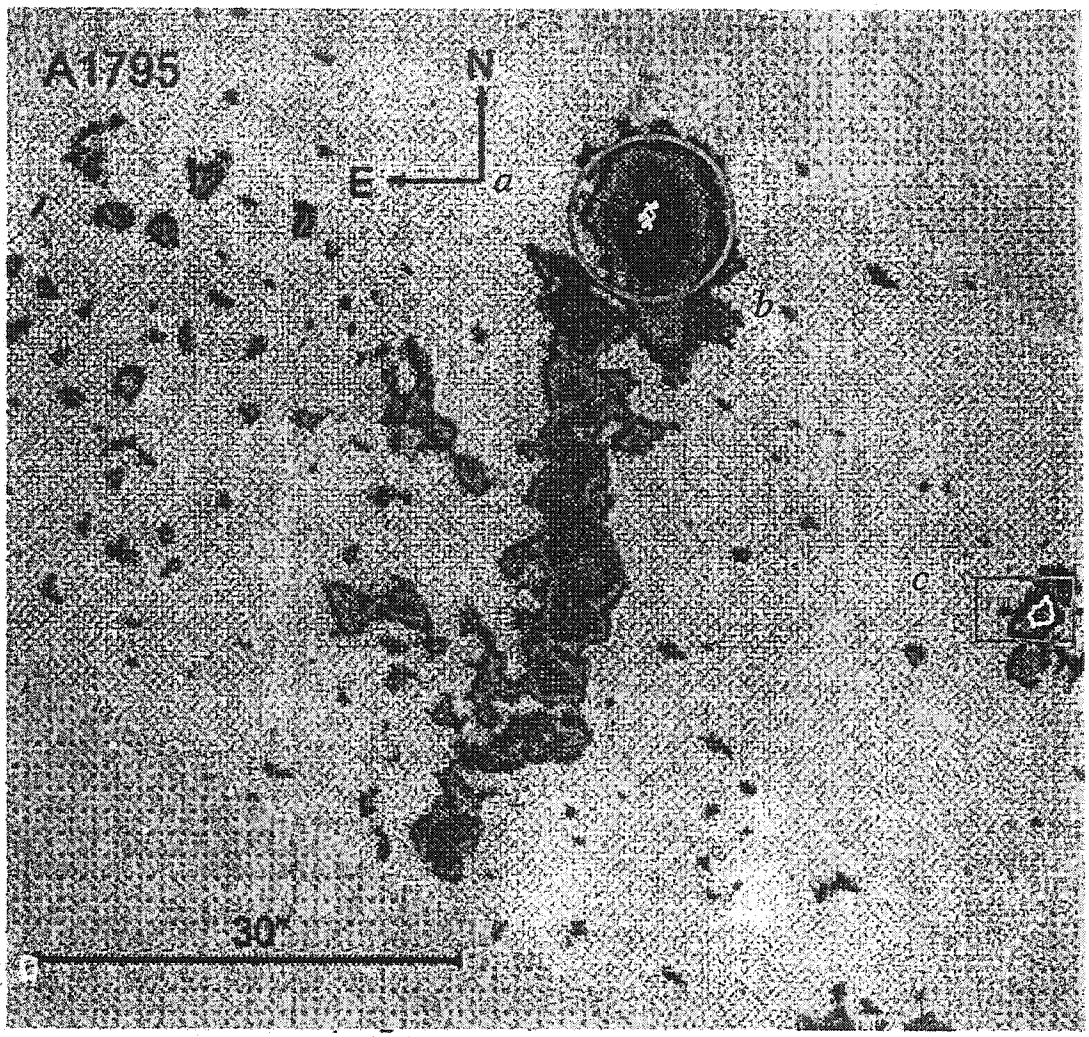

Figure 4.2: The H_2 emission is presented as contour overlays on the Hα image. Dark shades represent strong Hα emission. The optical extent of the CDG is shown as a light gray circle (radius = 5"). Adapted from McNamara (1996).

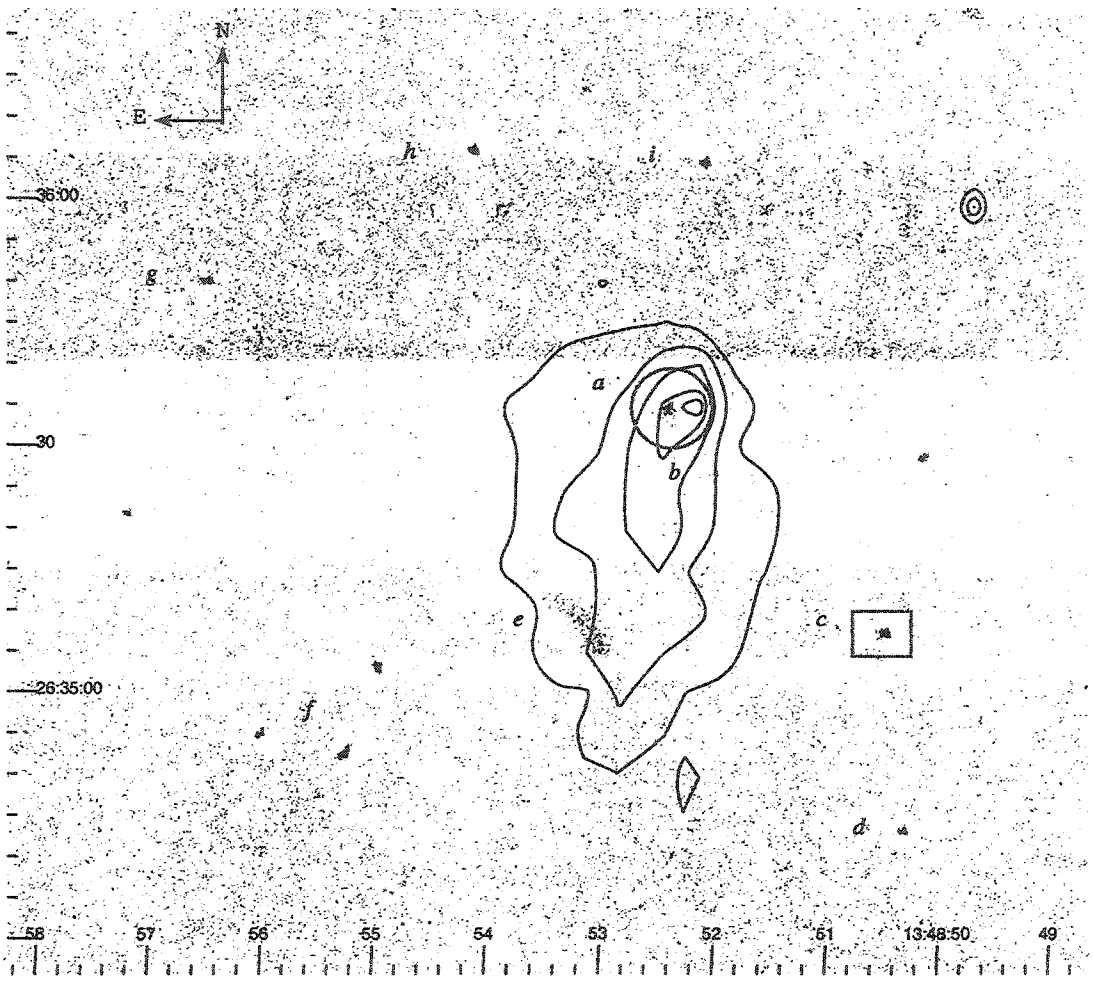

Figure 4.3: Chandra X-ray image contours (black) overlayed on the 2.0' by 2.0' field of view of H_2 emission. Dark features represent H_2 emission. The optical extent of the CDG is shown as a light gray circle (radius = 5") and there is a gray rectangle around Feature *c*.

excess attributed to young hot stars which emit much of their continuum flux in the UV. McNamara et al.(1996) infer that the amount of O[II] is negligible based on the amount of Hα emission found by Cowie et al.(1983). Thus the dark areas representing residual emission shown in Figure 4.4 originate from UV continuum emission. The UV filaments marked D, E and F correspond to the X-ray and Hα tails shown in Figure 4.1. Figure 4.5 shows the H_2 image with U-band residuals overlayed as contours. There is H_2 emission at the center of the cD galaxy and the bright H_2 emission found to the North East of the cD galaxy (Feature *h* of Figure 4.5) lies on top of a region which contains a UV excess, a sign that there has been recent star formation at these locations. The existence of hot stars and H_2 emission in these regions hints at the possibility that the hot stars may be a source of heating for the H_2 (see section 4.6).

4.3 Radio

For CFCs, imaging of radio lobes and optical spectra of the central galaxy has shown that approximately 90 percent have CDGs with associated AGN (Markevitch 2003). For non-CFCs, the percentage is closer to 30. This suggests that there is a relationship between the cooling flow and the AGN. In many CFCs, radio lobes are found in the same region as X-ray holes; X-ray and radio emission therefore appear to be anti-correlated. One explanation is that the radio emitting gas, rising because of its low density, push away the X-ray emitting gas creating these X-ray holes (Blanton, 2003).

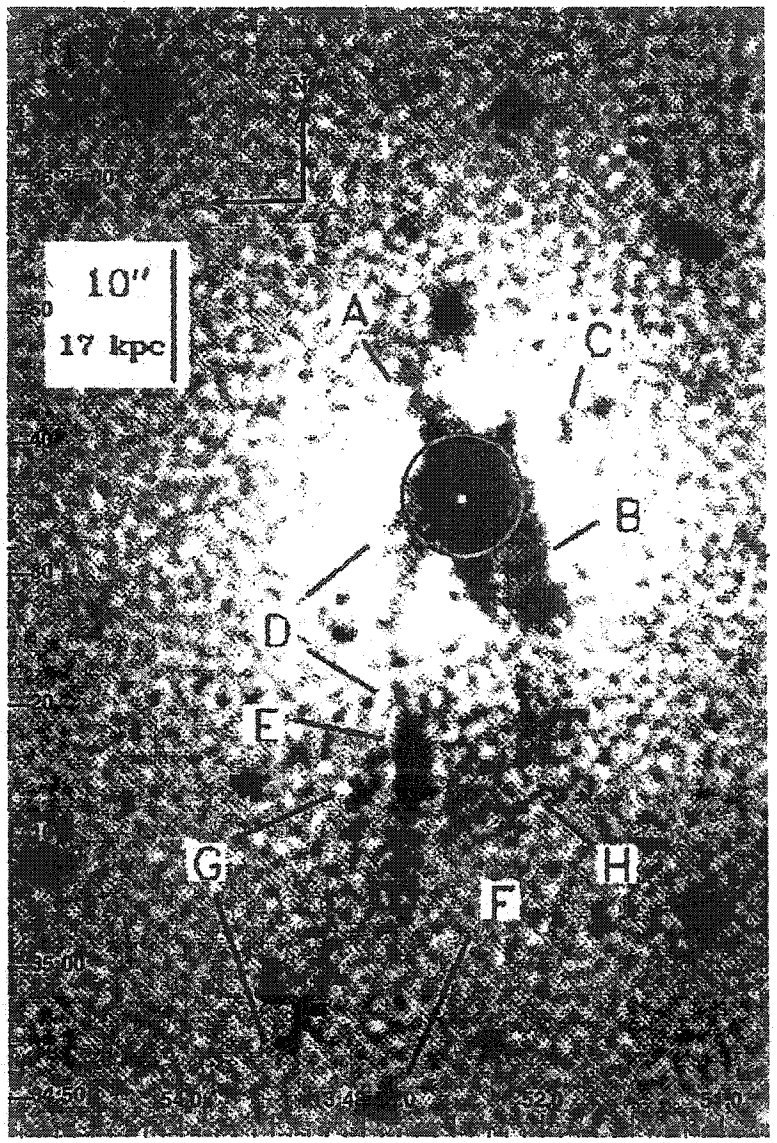

Figure 4.4: This figure shows a 1' by 1.5' field of view of prominent filaments that appear in the U-band once a model of the CDG has been subtracted off. Dark features represent the sites of UV excess. The optical extent of the CDG is shown as a light gray circle (radius = 5"). Adapted from McNamara (1996).

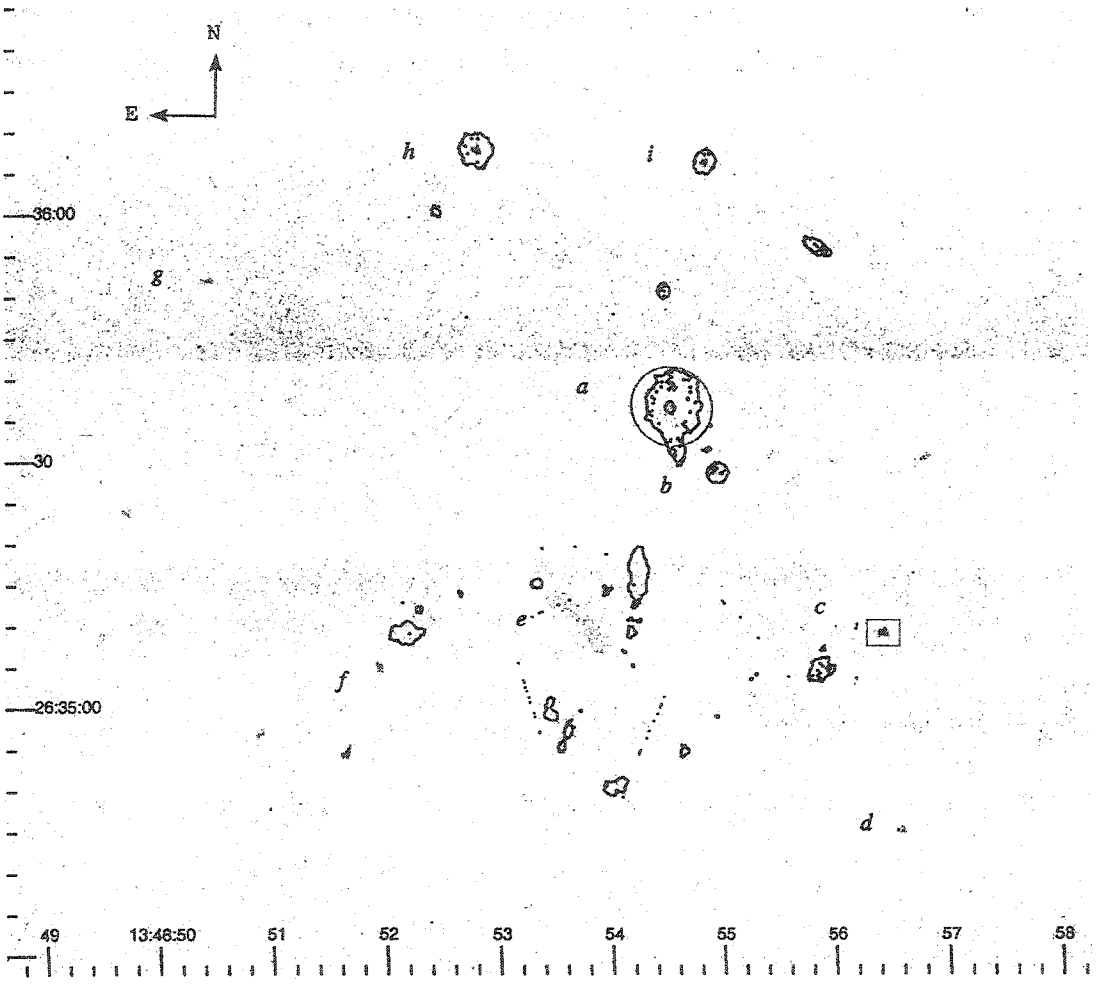

Figure 4.5: The U-band residual image is presented as contour overlays on a 2.0' by 2.0' field of view of the H_2 image. Dark features represent H_2 emission. The optical extent of the CDG is shown as a light gray circle (radius = 5"). Adapted from McNamara (1996).

Abell 1795 contains a double lobed FR I [1] radio source which extends 10kpc on either side of the CDG nucleus (McNamara et al. 1996).

The 3.6cm radio lobes overlayed on the smoothed Chandra X-ray image [2] are shown in Figure 4.6. Figure 3 of Pinkney et al.(1996) shows that the optical residual flux of the CDG (which will be compared to the H_2 emission in the following section) and radio emission are correlated. Figure 3.6 shows that our observations do not detect any substructure in the CDG. The radio lobes do not extend much further than the CDG (see Figure 4.6).

Pinkney et al.(1996) fit and subtract off isophotes from a a F555W HST image (V-band) of the CDG in Abell 1795 in order to generate a residual image. Their Figure 3 shows regions of emission and absorption in the optical residual image as well as overlayed contours of 3.6 cm radio emission. Their results support an increase in star formation by the radio source, as blue star clusters are found near the lobes and jets (Pinkney et al. 1996). We do not find any H_2 emission near the edge of the lobes, suggesting the H_2 emission is not related to the blue star clusters found by Pinkney et al.(1996). We also find that Feature *c* is 20" away from the edge of the radio lobes, suggesting that it can't be associated with the radio emission from the CDG.

[1] A Fanaroff-Riley type I radio galaxy (FR I) has smooth two-sided jets running into large-scale lobes. FR II galaxies are more luminous and hot spots are seen in the lobes.

[2] In this thesis, the same Chandra X-ray data for Abell 1795 is displayed in three different ways. Both Figures 4.1 and 4.6 show smoothed images, although they are displayed using different contrast levels. Figure 4.3 shows the non-smoothed version.

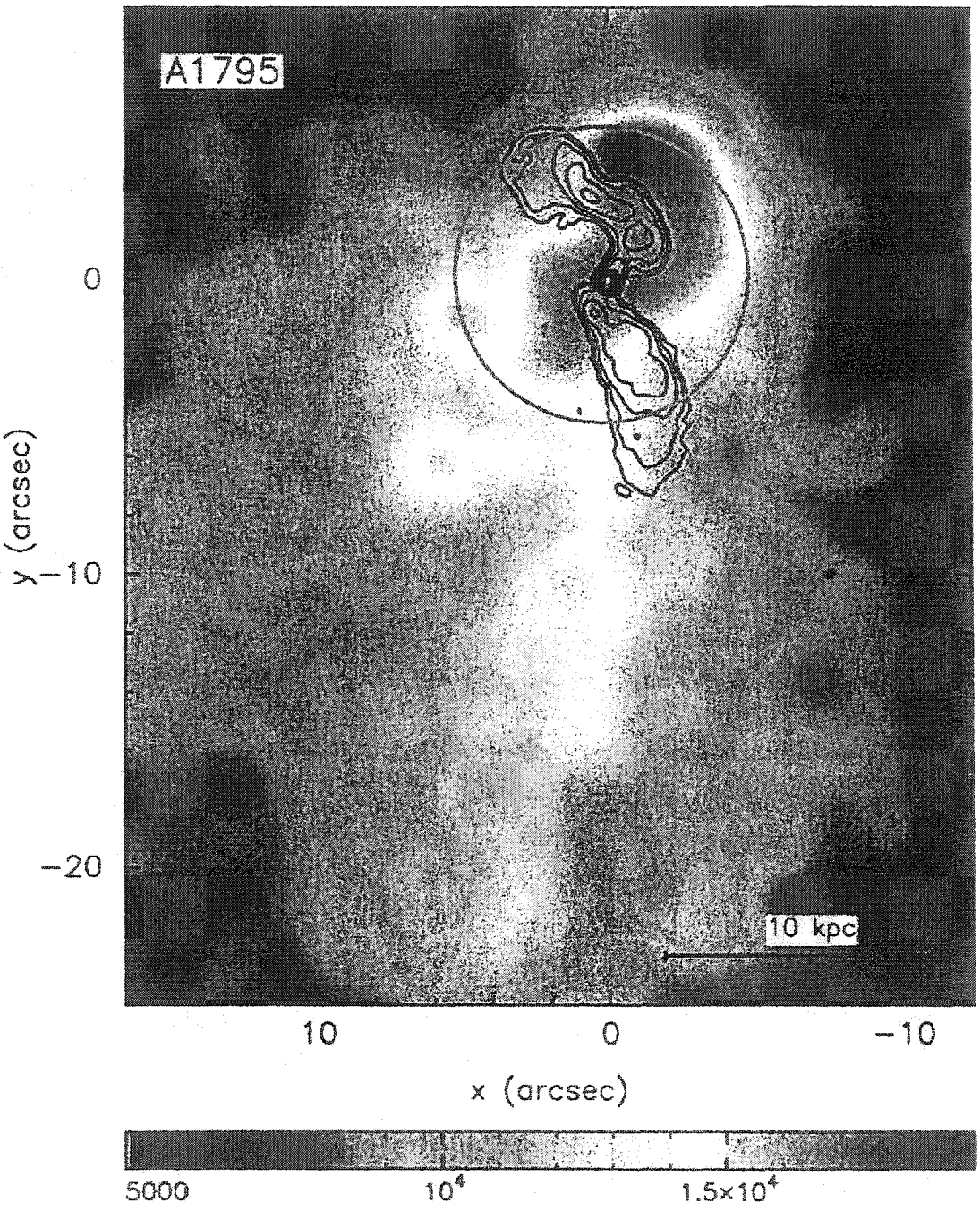

Figure 4.6: The 3.6cm radio lobes are shown as contours overlaying a smoothed 30" by 35" field of view X-ray image from Chandra. Dark features represent strong X-ray emission. The optical extent of the CDG is shown as a light gray circle (radius = 5"). Adapted from Fabian et al.(2001).

4.4 Optical HST Residuals of the CDG in Abell 1795

When the smooth profile of the optical emission of a galaxy is removed it can show many features that are associated with star formation such as spiral arms, rings or regions of absorption, probably caused by dust. We ask if the H_2 emission matches these residual features.

We generate our own residual image of the HST V-band image Abell 1795 by fitting a model using GIMFIT2D (Simard, 2000). Although in the end we find no difference in our results to those of Pinkney et al.(1996) described in the previous section, our results are based on a model fit (exponential disk + sersic bulge) thus having potential for a more accurate subtraction. The original image, model and residual image are shown in Figures 4.7-4.8, they show the same basic emission (dark) and absorption (light) features as Pinkney et al. (1996). Figure 4.8 shows the H_2 emission of the CDG as contour overlays on top of the V-band residuals. We do not find a relationship between the morphology of the molecular gas and the morphology of the residuals seen in the optical.

We include Figure 4.9 which shows the U-band residual image as contour overlays on the residuals of filter F555W in order to consider a relationship between the UV excess and the optical HST residual features. In Figure 4.9 Feature I is the elongated emission feature (extending about 5" away from the galaxy center) and is the main emission feature in Figure 4.4. Feature II is due to absorption in optical. Feature III is another site of UV excess and is labeled as Feature *b* in all other images. This

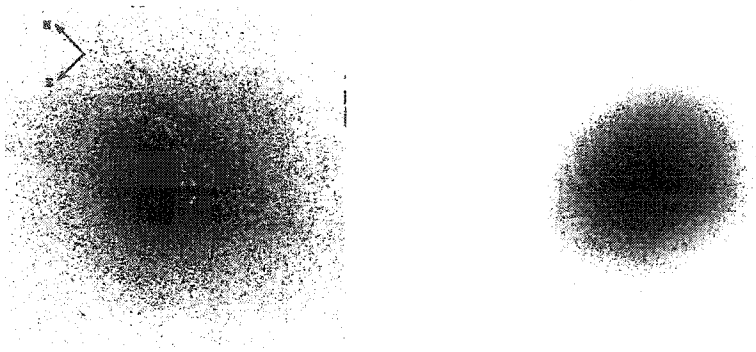

Figure 4.7: A 20 square arcsecond field of view of the HST image of the CDG of Abell 1795 in filter F555W is on the left. The model galaxy (same scale) produced by GIMFIT2D is on the right. Dark features represent emission.

figure is interesting as it shows that the U-band contours follow the largest emission feature from the GIMFIT2D residual image (Feature I). Emission features of the U-band residuals are sites of UV excess. As we have seen Feature I corresponds to an area of UV excess. Therefore the emission of Feature I in the residual of filter F555W (V-band) is likely due to young hot stars.

4.5 Non-CDG Molecular Hydrogen Detections

Before we leave the discussion of detections of H_2 emission in this cluster, we consider detections of H_2 emission in previously unexplored regions of a cooling flow cluster.

As the field of view for CFHT-IR is large (3.6' by 3.6') compared to the other telescope used to image molecular hydrogen in cooling flow clusters (HST), an interesting opportunity exists within this dataset that has not existed in previous observations of H_2 in CFCs. No other H_2 observations of a large field of view centered on the CDG in CFCs have been done, either spectroscopically or with imaging.

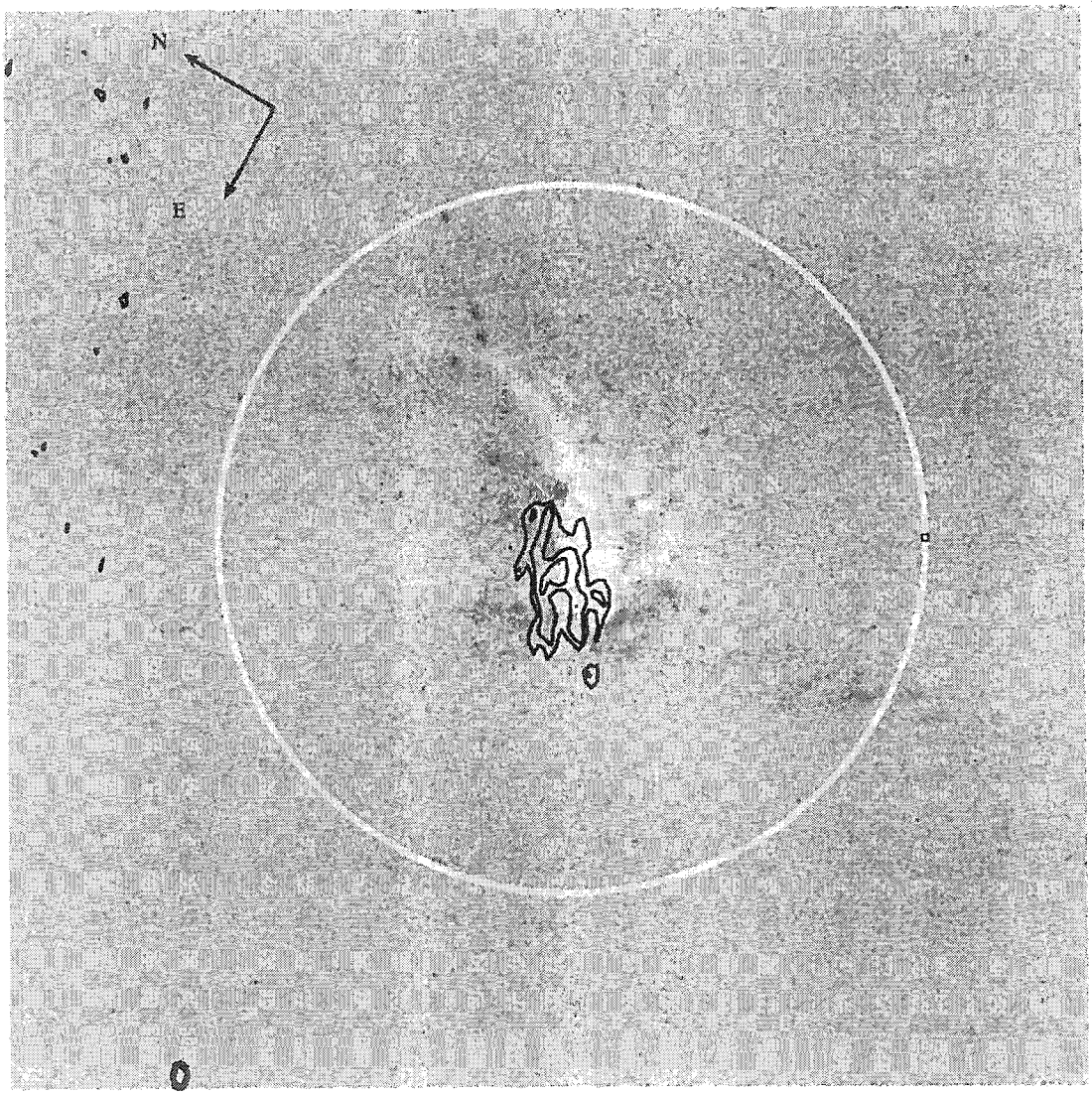

Figure 4.8: A 20 square arcsecond field of view of the GIMFIT2D residuals of the CDG of Abell 1795 is shown. Dark features represent emission and light features represent absorption. The H_2 emission is shown as black contour overlays and the light gray circle (radius = 5") shows the extent of the optical CDG.

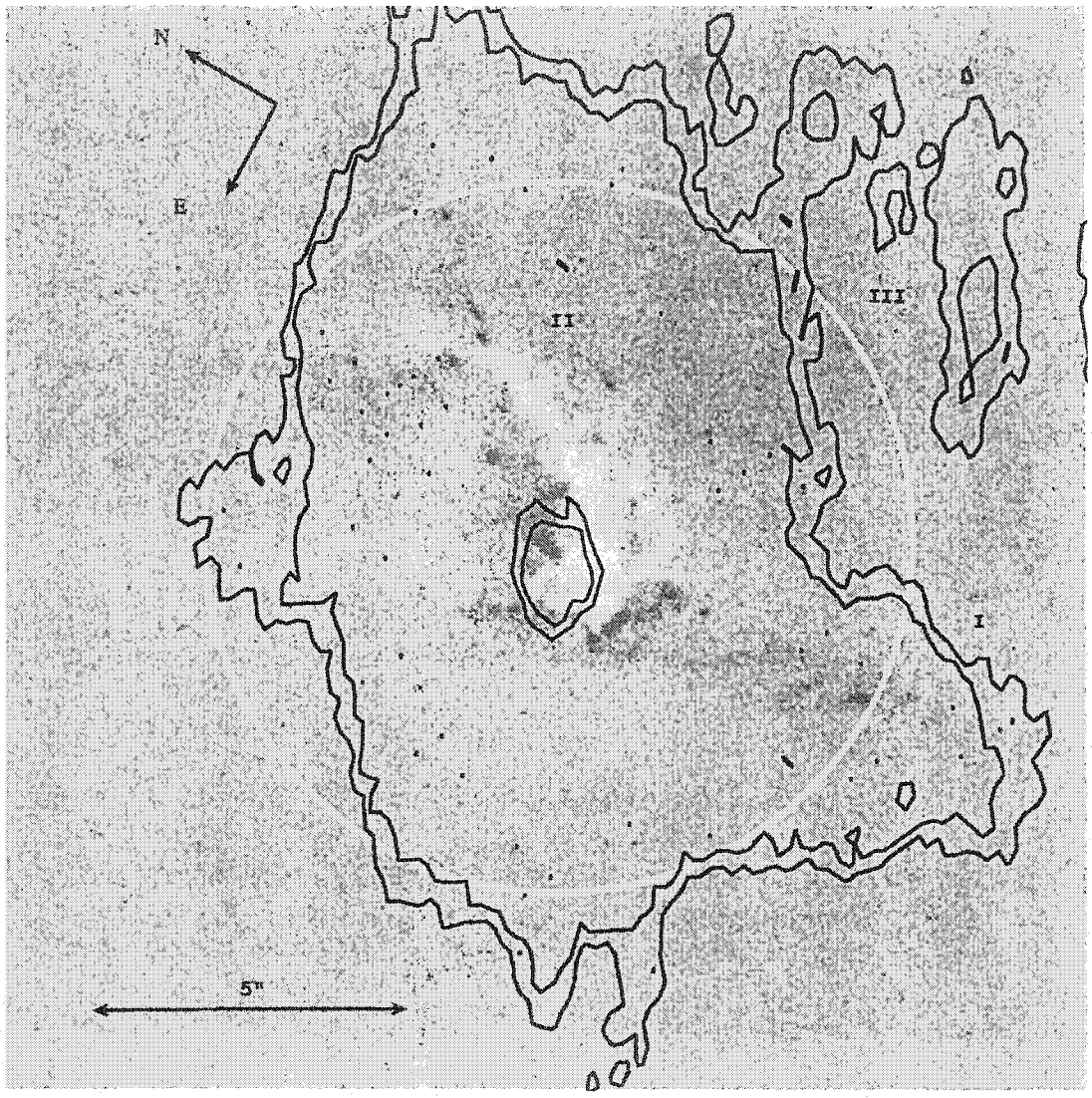

Figure 4.9: A 20 square arcsecond field of view of the GIMFIT2D residuals of the CDG of Abell 1795 is shown with the u-band residual image of McNamara et al.(1996) as black contour overlays. The contours on the upper left hand side of the frame (Feature III) correspond to Feature *b* in Figure 3.3.

In fact, other than broadband near-IR and optical photometry and some optical spectroscopy, not much has been published on the non-CDG galaxies of CFCs.

The brightest H_2 emission is expected to be seen in the central cluster galaxy and there exists only attempts to search for H_2 in the CDG itself (private communication, Donahue, 2003).

Using CFHT-IR's large field of view enabled the surrounding galaxies to be imaged. Although many of the surrounding galaxies disappeared when the continuum was removed, H_2 emission shows up in other regions of the image (Features *b*, *c*, and *f*-*i* of Figure 3.5) corresponding to galaxies, such as 2MASX J13485429 + 2636058 (which is Feature *h*) and 2MASX J13485050 + 2635068 (which is Feature *c*).

No information about the morphological type of Features *c* or *h* are found, but, there exists a V-band magnitude for Feature *c* (V=17.3) as well as a redshift (z=0.0612) for Feature *h*. By searching in the 2MASS (Two Micron All Sky Survey) catalogues we found a K-band magnitude of 13.5 for Feature *c* and 14.03 for Feature *h*. There are two possibilities for the cause of the emission seen in these galaxies. (1) It could be due to emission of something other than H_2, or (2) it could be due to H_2 emission. The continuum subtraction relies on the assumption that the KC image contains the emission line and the CO image contains only continuum. We do not have spectra for these galaxies, therefore it is possible that the continuum emission of these galaxies is bizarre and a different scale factor is required between the KC and CO filters before subtraction. It is also possible that other emission features lie in the wavelength range of the filters we used, or, that because the redshift of these galaxies is different than that of the CDG, the v=1-0 S(1) H_2 emission line

falls outside of the filter. In short, we do not know the redshift of Feature *c*, and objects with redshifts outside of 0.0603 and 0.0693 are not expected to be members of the cluster.

We give four reasons in support of the cause of remaining flux being because of the v=1-0 S(1) H_2 emission line. First, the redshift of Feature *h* places the H_2 emission line we desire within the KC filter's bandpass. Second, although many of the galaxies disappeared after continuum subtraction, these remained. Third, they are strong signals (especially Feature *c*) and are condensed as is the H_2 emission in the CDG. And fourth, there is emission in the Hα image that is in the same place as that of Feature *c*.

If H_2 emission exists in non-CDGs this presents a problem for the idea that the molecular hydrogen is due to the cooling flow itself. All the emission we found is still inside the cooling radius (181 kpc for Abell 1795, Grenatcher et al. 1999). However, if emission were found outside of the cooling radius, where the cooling flow does not occur, the molecular gas would not have been deposited by the cooling flow. Rather, detections of molecular gas in the non-CDGs of CFCs beyond and near the cooling radius, are consistent with an alternate source for the molecular gas.

4.6 Energetics

Our data show that molecular gas and evidence of new stars, not generally found in elliptical galaxies, exist in the galaxies near the center of Abell 1795. This supports the picture that cooling flow clusters have a reservoir of cold gas which may form

stars (H_2, UV excess and Hα alignment). The fact that the H_2 flux is too high to be due to the cooling flow (see Chapter 3), suggests that the H_2 is reheated to temperatures above 1000K. We ask which H_2 reheating mechanisms are consistent with our results.

Possibilities for exciting the H_2 gas include shocks, and UV emission from hot stars and heating due to an AGN.

Heating due to fast shocks can be ruled out or supported depending on the Hα/H_2 ratio (Donahue et al. 2000). Previous observations of the Hα/H_2 v=(1-0) S(1) emission line ratio in other CFCs find numbers of 1-10 which are too low for shock heating. For shock heating the ratio should be greater than 30 (Donahue et al. 2000). We use our results of the flux of H_2 v=(1-0) S(1) with a flux for Hα in Abell 1795 that has been determined by Baker, et al.(2003). Within an aperture radius that is about seven times larger than that used for the H_2 flux in this thesis, the Hα is $2.5\text{x}10^{-17}$ W/m^2. Thus an upper limit for the Hα/H_2 ratio is found to be 13. Since the upper limit is smaller than the value required for heating due to fast shocks, our data rules out this heating mechanism.

Wilman et al.(2002) dismiss heating by hot stars because of a lack of H_2 v=(2-0) lines in the H-band spectrum. However, others still explore this as a possibility. A filamentary, diffuse morphology may indicate heating from hot stars (Donahue et al. 2000). A region containing a UV excess is found to be coincident with H_2 emission in galaxies (Features *b*, *h* and *i*) surrounding the CDG, as well as for the CDG itself, supporting the claim of heating due to hot young stars. However, the H_2 emission data does not show any filamentary structure expected from heating due to hot

stars and there exists no hint of molecular hydrogen in the region hypothesized to be a cooling wake. If a faint filamentary structure exists in H_2, a higher signal to noise image of H_2 (we have a 5σ detection at the center) will reveal it. Also the UV excess and residuals from the optical HST image seem to be correlated. They both follow extended emission (Feature III in Figure 4.9), and the peak of all 3 sources of emission are centered at the same location, alluding to a history which may connect the three.

Figure 3.6 shows that the brightest H_2 emission exhibits a condensed morphology and therefore suggests the excitation mechanism to be due to the AGN. AGN heating is also consistent with our observations of H_2 emission outside of the CDG as the galaxies surrounding the CDG could also contain AGN of their own.

Chapter 5

Conclusions

In this work the morphology of the emission from different wavebands in the cooling flow galaxy cluster Abell 1795 is investigated.

In Chapter two, we search for correlations between the visual and X-ray emission and find that the only CDG of our sample of CFCs for which alignment was able to be determined was Abell 1795. The morphology of the Cluster's X-ray gas is however very interesting and may be due to the action of a cooling wake, although other possibilities exist. Ram pressure stripping of the radio source with the ICM or evaporation of cold gas stripped from the CDG are other options.

Therefore, in Chapter three we look for other evidence that might support the claim that the X-ray wake occurring from the action of the cooling flow. If the X-ray gas cools directly through 1000K molecular hydrogen can form and emit at the IR wavelength of 2.12μm. We therefore search for molecular hydrogen emission at this wavelength.

We find the H_2 flux from the v=1-0 S(1) emission line of the CDG is 1.93 +/- 0.79×10^{-18} W/m^2, a value which is of the same order as that calculated from the spectroscopic results of Jaffe et al.(2001).

When the morphology of the H_2 flux is compared to emission at other wavelengths we uncover clues as to the nature of the gas. The peak H_2 emission exists

in the central few arcseconds of the optical residuals of the CDG of Abell 1795. It appears at the center of the peak emission of the Hα image as well as the U-Band image, which are both tracers of emission from hot stars. It is also located off the peak of the X-ray emission, where the peak of the cooling flow is expected. The Hα, X-ray and U-band images all show evidence of a tail to the south of the CDG, which is not apparent in the H_2 emission. Our data agree with the hypothesis that the cooling flow and the H_2 emission are not directly related (Donahue et al. 2000).

The most exciting result of this work is the first detections of molecular hydrogen in a non-central galaxy in a cooling flow cluster. We give reasons why caution should be observed when classifying emission remaining in many of the cluster members to be strictly from H_2 emission. However, the following conclusion is made: Features *c* and *h* of Figure 3.5 likely have the first detections of molecular hydrogen, either spectroscopic or imaging, in a non-central galaxy of a cooling flow cluster. This finding also supports a non-cooling flow origin for the molecular gas. H_2 emission would be expected mostly in the center of the CDG if it was a direct result of the cooling ICM.

The value of the amount of H_2 emission in the CDG is too large to be due to just simple cooling of the X-ray gas; we require a large source of H_2 being reheated up to temperatures of 1000K. We are able to obtain an upper limit to the ratio of Hα/H_2 of 13, which rejects the notion of reheating due to shocks (recall shock heating requires a ratio of at least 30, Donahue et al. 2000). The energetics of the gas in the CDG point to heating from hot stars, as the Hα/H_2 ratio is most consistent with UV heating from hot stars. However, the morphology of the H_2

emission paints a different picture; our image does not reveal a diffuse structure in the H_2 emission, rather the emission looks condensed, implying reheating by an AGN.

The data we have analyzed in this thesis uncovers the existence of H_2 emission in the CDG as well as in Features *c* and *h*. In terms of the big picture, these results imply reheating of molecular hydrogen by an AGN or hot stars, and strengthen the case for a non-cooling flow origin of the molecular gas. In the classical picture of cooling flows, X-ray gas simply cools and condenses to form molecular gas and stars in the CDG. The numbers do not support the cooling flow scenario; rather, it seems the molecular gas may not be directly linked to the cooling flow.

Still puzzling is (1) the source of the H_2, especially as H_2 is now seen away from the CDG, yet not in the cooling wake discussed in Chapter 2; (2) the nature of the tails seen in Hα and X-ray; (3) the relationship between the X-ray emitting gas and the radio emission. We have been able to rule out fast shocks as a reheating mechanism for Abell 1795, but deeper observations are needed in order to discriminate between heating due to an AGN or due to UV radiation from hot stars.

5.1 Future Projects

One possible project for the future that could help solve some of the puzzles which still exist is further analysis of the small non-central galaxies in H_2. Follow up observations should concentrate on detecting molecular gas beyond the cooling radius and an obtaining spectra of these galaxies. It would also be interesting to see if

$H\alpha/H_2$ ratios for these galaxies were the same as for the CDG. If only the galaxies inside the cooling radius were heated by hot stars, this would lend support to the theory that hot stars were related to the cooling flow.

Observations of the clusters Abell 644, Abell 400 and AWM7 (PI Louise Edwards) are planned for November, 2003. With these observations there will be a total of seven clusters imaged in molecular hydrogen, four with information of molecular hydrogen in non-CDG galaxies. The use of Chandra rather than Einstein or Rosat data will help to determine the relationship between the different wavebands as the pointing accuracy is much higher.

Finally, once the Space InfraRed Telescope Facility (SIRTF) becomes publicly available in 2004, we hope more of the questions regarding the excitation mechanism of H_2 in CFCs will be answered. Line ratios of different molecular hydrogen transitions that are currently hidden from us due to atmospheric absorption may reveal the nature of the excitation of this gas. If the heating is from UV radiation from hot stars, dust should re-emit the UV radiation in the Far-IR, and this emission should also be detected by SIRTF (Donahue et al. 2000).

Appendix A: Original CFC Lists

Table 5.1: List of Cooling Flow Candidates

Cluster	Fabian et al.(1994) $\dot{M}$ ($M_\odot$/yr)	White (2000) $\dot{M}$ ($M_\odot$/yr)	Peres et al.(1998) $\dot{M}$ ($M_\odot$/yr)	Most Recent $\dot{M}$ ($M_\odot$/yr)	Comment
A1835		1978		230	Schmidt et al. 2001
A2219		989		<200	Houck et al. 2001
A1942		817			
A1774		732			
PKS0745-191	702	552	900		
A478	570	636	570		
A2597	480t	259	273	50	McNamara et al. 2001
				40	Oegerle et al. 2001
A1795	478	453	430	>10	Fabian et al. 2001b
				150	Tamura et al. 2001
A3112	430	161	395		
A2029	402	0	555	100	Stocke and Lewis 2000
A1775		366			
A990		348			
A644	326	0	200	214	Brauer and Sarazin 2000
A3921		319			
Hydra-A	315		280	29	David 2001
A586		271			Nothing
A85	230	147	155	108	Kempner and Sarazin 200
					Merger
A2390		234		250	Allen et al. 2001
A2142	188	505	320	69	Markevitch 2000
Cygnus-A	187	564	235	10	Wilman et al. 2000
A426	183	671	490		CF, Peterson et al. 2001
A2151		173			
A1689	164t	118	570		
MKW3s	151	138	140		
A2199	150	130	160		
2A0335+096	142	75	275		
A4059	124	51	120	27	Heinz 2002

continued on next pag

continued from previous page

Cluster	Fabian et al.(1994) $\dot{M}$ ($M_\odot$/yr)	White (2000) $\dot{M}$ ($M_\odot$/yr)	Peres et al.(1998) $\dot{M}$ ($M_\odot$/yr)	Most Recent $\dot{M}$ ($M_\odot$/yr)	Comment
A539		120			
A496	112	138	95	$70h^{-1}$	Tamura et al. 2001
A2052	90	120	112	120	Blanton et al. 2001
A1656		87			
A2811		87			
A2244	82t		244		
A3571	79	130	75	80	Navalainen 2001
A3627		76			
Ophiuchus	75	0	80		
A2319	66t	431	12t	NCF	Gruber and Raphaeli 2002
3C129	61			NCF	Krawczynski 2002
A2107		57			
A3526		56			
A2147	54t	119			
A3558	50	219	40t		
A262	47	26	27		
A3562	45	167			
A2063	45	99	37		
A2670		44			
AWM7	42	29	30	CF	Furusho et al. 2001
MKW4s		25			
A754	24	218	1t		
A400		24		<10	Eilek and Owen 2002
A119	23t	52	0t		
A970				20	Sodre 2001
A1644	19t		11	M	Srinivasan and Mohr
A2657		19			
Centaurus	18		26	CF	Furusho et al. 2001
MKW9		14			
A401	12	326t	42t		
AWM4		11			
Virgo	10	5	30	NCF	Finoguenov and Jones 2001,
A3266	10	145	2	M	Flores et al. 2000
A1060	9	6	11	CF	Furusho et al. 2001
A576	6t	0	3		
Tri.Aust.	0	161	33		
Coma	0t		0t		
A3667	0t	196	0t	M	Vikhlinin 2001
A2256	0t	439	0t		
A1651		231	138		

continued on next page

continued from previous page

Cluster	Fabian et al.(1994) $\dot{M}$ ($M_\odot$/yr)	White (2000) $\dot{M}$ ($M_\odot$/yr)	Peres et al.(1998) $\dot{M}$ ($M_\odot$/yr)	Most Recent $\dot{M}$ ($M_\odot$/yr)	Comment
A1367	0t	57	0t		
A399	0t	368	0t		
A3158	0t	292	25t		
A2065	0t	273	13		
Klemola44		55	87		
A2204		984	847		
A1650	0	115	280		
A3532	0t		0t		
A3391	0t	131	0t		
A2255	0t	122	0t		
A1736	0t	79	1		
A370		0			
A521		0		M	Ferrari, 2001, conf
A548		0			
A611		0			
A665		56		M	Markevitch 2000
A697		0			
A773		0			
A854		0			
A963		0			
A1068		0			
A1204		675			
A1246		0			
A1413		210			
A1553		2237			
A1576		0			
A1682		0			
A1704		7			
A1763		0			
A1772		0			
A1851		0			
A1895		0			
A1914		256			
A1995		0			
A2034		400			
A2104		0			
		0		M	Makevetich and Vikhlinin 200
A2218		450		M	Machacek, 2002
A2261		0			
A2440		0			

continued on next pag

continued from previous page

Cluster	Fabian et al.(1994) $\dot{M}$ ($M_\odot$/yr)	White (2000) $\dot{M}$ ($M_\odot$/yr)	Peres et al.(1998) $\dot{M}$ ($M_\odot$/yr)	Most Recent $\dot{M}$ ($M_\odot$/yr)	Comment
A2634		0		NCF	Eilek and Owen 2002
A3221		465			
A3376		0			
A3921		319			
CL0016		0			
SC1327		90			
Zw3146		2061			

The symbol "t" is used if a cluster is rejected because it has a cooling time is greater than the age of the Universe. NCF refers to a cluster that has been published as Not being a Cooling Flow. If the cluster has been published as being a cooling flow, the letters CF are used. If the cluster's cooling flow has been disrupted by a merger, an "M" is used to signify this.

Appendix B: Observation Log

GFH Program: C21

UT	File Name	Object Identification	Filter	Integ. Time	Acq. Mode	Number Images	Airmass	Comments
	696705f	flat	KC	10s	Cube	10		(B) Flats. lights on - lights off. ON (Cal)
	696706f	flat	KC	10s	Cube	10		lamp B " " " " OFF
	696707f	flat	CO	30s	Cube	1		" " " " ON
	696708f	flat	CO	30s	Cube	10		" " " " ON
	696709f	flat	CO	30s	Cube	10		" " " " OFF
	696710d	Darks	Cold Blank	2s		30		Cold Blank Filter
	11d	"		10s		10		
	12d	"		30s		96		neg. values(?)
	13d	"		60s		65		
	14d	"		200s		36		
	15d	"		400s		33		
	696716d	"		600s		3		
	696717	star	KC	10s		1		6th mag. star.
05:06:00	18	"	"	2s		1		too bright to focus
	19	FS18		10s		1		BAD. Frame.
	20	FS18		10s		1		
	21	Focus.		20s				Focus on FS18.
	22			2s				focus on bright star. CAF: 2s 18 (2029)
	23							
	24		KC	20s		1		Check → 10000 counts. Seeing: 1.1
	25	FS18	KC	20s		1		Check → 10 000 counts
06:06:07	26	FS18	KC	40s	Cube	6	1.07	Position 1 Seeing: 0.696.
	27	FS18	KC	40s		6	1.03	2 0.705
	28	FS18	KC	40s		6	1.04	3 counts: 18 000. 0.833
06:20:07	29	FS18	KC	40s		6	1.06	4 0.678

GFN Program :

UT	File Name	Object Identification	Filter	Integ. Time	Acq. Mode	Number Images	Airmass	Comments
06:10:31	696730	FS18	KC	40s	Cube	6	1.08	position 5 counts 18000 seeing: 0.676
	696731	star	CO	10s			1.10	focus. T: 0 2021
	696732							
	33							focus.
	34	star.	CO	10s		1	1.811	2021 focus seeing: 0.811
	35	FS 18	CO	60s		1		count 10 000
	36	FS18	CO	60s	Cube	4	1.13	position 1 counts. 13000 seeing: 0.59
	37	FS18	CO	60s	Cube	4	1.14	2 counts 12000 0.66
	38	FS18	CO	60s	Cube	4	1.14	3
	39	FS18	CO	60s	Cube	4	1.15	4 counts 11000
	40	FS18	CO	60s	Cube	4	1.16	5 counts 14000 0.68.
07:24:09	41	A1795	CO	360s		1	1.39	might be weird. (aborted ½ way through)
	42	A1795	CO	360	Cube	1	1.31	pos. 1 } 1st time thru dithers. (out of 9)
	43	"	"	"	"	"		2
	44	"	"	"	"	"		3
08:06:45	45	"	"	"	"	"	1.24	4
	46	"	"	"	"	"	1.22	5
08:18:48	47	A1795	CO	360	Cube	1	1.20	pos. 1 } 2nd time 4 5
	48	"	"	"				2 1 25"
	49	"	"	"				3 3 2
	50	"	"	"			1.13	4
	51	"	"	"				5
	52	A1795	CO	360	Cube	1	1.11	pos 1 } 3rd time
	53	"	"	"	"	"	1.09	2
	54	"	"	"	"	"	1.09	3

CFH Program :

UT	File Name	Object Identification	Filter	Integ. Time	Acq. Mode	Number Images	Airmass	Comments
	696756	A1795	CO	360	Cube	1	1.08	pos. 4 } 3rd time.
	56	"	"	"	"	"	1.06	5
09:26:02	696757	A1795	CO	360	Cube	1	1.06	pos. 1
	58	"	"	"	"	"	1.05	2 4th time.
	59	"	"	"	"	"	1.04	3
	60	"	"	"	"	"	1.03	4
	61	"	"	"	"	"	1.03	5
09:58:53	696762	A1795	CO	360	Cube	1	1.02	pos. 1
	63	"	"	"	"	1	1.02	2 5th time.
	64	"	"	"	"	1	1.01	3
	65	"	"	"	"	1	1.01	4
	66	"	"	"	"	1	1.01	5
10:31:56	696767	A1795	CO	360	Cube	1	1.01	pos. 1 6th
	68	"	"	"	"	"		2 time.
	69	"	"	"	"	"		3
	70	"	"	"	"	"		4
	71	"	"	"	"	"	1.01	5
11:05:45	696772	A1795	CO	360	Cube	1	1.01	pos. 1 T = -1
	73	"	"	"	"	"	1.02	2 7th time.
	74	"	"	"	"	"	1.02	3
	75	"	"	"	"	"	1.03	4
	76	"	"	"	"	"	1.03	5
11:31:50	696777	A1795	CO	360	Cube	1	1.03	pos 1
	78	"	"	"	"	"	1.05	2 8th time.
	79	"	"	"	"	"	1.05	3 tried to abort here.

CFH Program :

UT	File Name	Object Identification	Filter	Integ. Time	Acq. Mode	Number Images	Airmass	Comments
12:02:4	696780.0	A1795	CO	360s	Cube	1	1.06	pos. 4 (8th time.
	81.0	"	"	"	"	"	1.07	5
12:16:31	696782.0	star.	KC	2s	Cube	1	1.09	9.2 arc check focus for (not Zw 29) FWHM: OUT of focus!
	696783.0	star.	KC	4s				FOCUS CAF (4/10)
12:26:03	696786.0	star.	KC	9s	Cube	1	1.11	exp. @ 7058. FWHM 3.00 arc sec 2.63?
	87.0	"	KC	4s	"	"	1.11	@ 7069
12:	696788.0	A1795	KC	246s	Cube.	1	1.12	Focus is (7058) counts: 9000.
12:37:03	696789.0	A1795	KC	246s	Cube	1	1.13	pos. 1
	90.0	"	"	"	"	"	1.14	2
	91.0	"	"	"	"	"	1.15	3 (1st (out of 4.)
	92.0	"	"	"	"	"	1.16	4
	93.0	"	"	"	"	"	1.17	5
13:00:0	696744.0	A1795	KC	246s	Cube	1	1.18	pos 1
	95.0	"	"	"	"	"	1.20	2
	96.0	"	"	"	"	"	1.22	3 (2nd some light clouds to west.
	97.0	"	"	"	"	"	1.23	4
	98.0	"	"	"	"	"	1.24	5
	696799.0	A1795	KC	246s	Cube	1		pos. 1
								2
								3 (3rd
								4
								5
	696799.0	A1795/star.	KC	10s	Cube	1	1.26	check focus of 2058 FWHM: Saturated
	696800.0	A1795/star	KC	10s	Cube	1		" " " 2030 FWHM: Saturated

GFH Observer:

Program:

CFHT IR OBSERVING LOG

UT	File Name	Object Identification	Filter	Integ. Time	Acq. Mode	Number Images	Airmass	Comments
	696 801o	A1795/star	Kc	2s	Cube	1		2030 → blades bad. Not set.
	696802o	A1795/star	Kc	2s	Cube	1		2058 Guide 7.99.
13:27:00	696803o	A1795	Kc	24s	Cube	1	1.27	pos 1 counts: 10050
	804o	"	"	"	"	"	1.29	2 not much cloud.
	05o	"	"	"	"	"	1.31	3
	06o	"	"	"	"	"	1.33	4 counts: 9000.
	07o	"	"	"	"	"	1.35	5
13:49:08	696808o	A1795	Kc	24s	Cube	1	1.38	pos 1
	09o	"	"	"	"	"	1.42	2 4th.
	10o	"	"	"	"	"	1.43	3
	11o	"	"	"	"	"	1.45	4
	12o	"	"	"	"	"	1.46	5 final airmass 1.51
14:13:46	696813o	FS27	Kc	22s	Cube	1	1.06	
	696814o	FS27	Kc	60s	Cube	4	1.06	pos 1
	15o	"	"	"	"	"	1.06	
	16o	"	"	"	"	"		
	17o	"	"	"	"	"		
	696818o	FS27	CO	60s	Cube	1		FOCUS: 2021
	696815o	FS27	CO	20s		3		
	696815o	FS27	Kc	60s	Cube	4	1.07	2
	16o	"	"	"	"	4	1.07	3
	17o	"	"	"	"	4	1.08	4
	696818o	FS27	"	"	"	4	1.08	Change filter, change focus, Change IT: 5
14:49:16	696819o	FS27	CO	90s	Cube	1	1.09	(change filter, focus, IT Point. focus: 2021.
	696820o	FS27	CO	200s	Cube	1	1.09	10000 counts:

CFH Program :

UT	File Name	Object Identification	Filter	Integ. Time	Acq. Mode	Number Images	Airmass	Comments
14:56:39	69682[1]0	Fs27	CO	360	Cube	1	1.10	pos. 1 Counts : 6700
	220	"	"	"	"	"	1.11	2
	230	"	"	"	"	"	1.12	3
	240	"	"	"	"	"	1.13	4
	———	corrupted	———	———	———	———	———	5 ———
	696825f	flat	CO	30s	Cube	10		Lamp B ON 15000 counts
	26f	"	"	"	"	"		" " OFF 1200 counts
	CORRUPTED	———	———	———	———	———	———	———
	696829f	flat	KC	10s	Cube	10		Lamp B ON 29000 counts (sat)
	30f	"	"	6s	"	"		" " ON 17000 counts
	31f	"	"	"	"	"		" " OFF 1000 counts.
	696832d	Darks	cold blank					same as first part of night.
	48d							neg. values → ask olivier.

Appendix C:

Observing Proposals

CFHT Proposal

Date: March 26, 2002Category: Structure and Dynamics of Galaxies Proposal:

CFHT
OBSERVING TIME REQUEST
Semester: 2002B Agency: Canada

1. Title of the Program *(may be made publicly available for accepted proposals)*:
Seaching for Molecular Hydrogen in Cooling Flow Clusters Abell 85, Abell 2319 and Abel

2. Principal Investigator: Louise Edwards
Postal address: Saint Mary's University, Astronomy and Physics Dept. Halifax, NS B3H 3C3
Fax: Phone: E-mail:

3. Co-Investigators:

Francine Marleau	Institute: Saint Mary's University	E-mail:
Gary Welch	Institute: Saint Mary's University	E-mail:
Nick Tothill	Institute: Saint Mary's University	E-mail:

4. Summary of the Program *(may be made publicly available for accepted proposals)*:
We propose to image a sample of three cooling flow clusters (Abell 85, Abell 2319 and Abell 644) in H_2 a set of filters with CFHTIR. Cooling flows are produced by the cooling of the hot Intracluster Mediun eventually this gas cools into a molecular state, where it can radiate in the near-IR. However, the mol component of the cooling flow and its excitation are still poorly understood, largely due to the pauc observations. By covering a range in redshift and cooling flow mass flux, we will be able to (1) measu H_2 line flux, (2) find how this H_2 line flux trends with redshift, and (3) measure the spatial extent emission. This study is part of our plan to undertake a full spectroscopic study of cooling flow clusters 8m class telescopes.

5. Summary of the Observing Run Requested:

Instrument	Detector	Moon (d)	Filters	Gr
CFHTIR	N/A	14	Br-Gamma, H2 v=2-1 s(1), K Continuum, CO	

Time Req.	Service/Queue?	Queue Mode	Image Quality	Opt. LST	Min. LST	Max.
3 nights	No	—	—	03:00	01:00	06:

6a. Is this a joint proposal? NO 6b. If yes, total number of nights or hours requested from all agencies? —
7a. Is this a Thesis Project? YES 7b. If yes, indicate supervisor: Dr. F. Marleau

8. Special instrument or telescope requirements:

9. Scheduling constraints:

10. Scientific Justification *(science background and objectives of the proposed observations: 1 page maximum)*:

X-ray observations of nearby clusters of galaxies show sharp peaks as dense gas in the center of the cl cools. This cool gas, unable to support the outer part of the Intracluster Medium, flows towards the c of the cluster. The result is a long-lived stable 'cooling flow' (see the review by Fabian 1994). In the central regions of these flows, the gas is expected to become molecular. We expect H_2 emission whi characteristic of molecular gas at temperatures of order 1000K. Near-infrared spectra of galaxies assoc with three cooling flow clusters (CFCs) were obtained by Falcke et al (1998). They found that these (are strong H_2 emitters. More recently, Donahue et al (2000) observed a sample of three CFCs (one of v from the sample of Falcke et al) with redshifts making the H_2 emission line appear in NICMOS filters. also found strong H_2 emission.

However, when the inferred mass cooling rate from X-ray observations (Jaffe and Bremer 1997) is comp to the one inferred from H_2 emission, they disagree. The rate found from H_2 is larger. Surprisingly, sea for CO emission from the molecular gas have found only small amounts (eg Braine and Dupraz 1994 lc at 8 CFCs). One explanation of this discrepancy is that the molecular gas, once formed, is reheated by mechanism, such as shocks or reionisation of the gas by an AGN (Bohringer 2002) or a massive star in the central galaxy (Edge 2001). This highlights the fact that the H_2 emission from CFCs is still p understood. As well, there are few detections of H_2 in the literature, so there is little understanding c systematic properties of H_2 emission in cooling flows - Do all cooling flows show H_2 emission? Doe emission strength correlate with cooling flow emission or optical emission lines such as Hα? Does it cor with redshift? A larger sample of H_2 observations of CFCs may be able to answer these questions.

We propose to observe a sample of three CFCs using a set of filters with CFHTIR. This survey is part c plan to undertake a full spectroscopic survey of CFCs at a variety of redshifts using 8m class telescope Gemini). This imaging study is both preliminary and complementary. It is preliminary in that the H flux and how this flux trends with redshift will be useful to the spectroscopic survey, and it is compleme as the spatial distribution of the H_2 is difficult to obtain with only spectroscopic observations.

Our sample of CFCs was taken from the B55 flux-limited sample of Edge et al (1990), with optical counter and further X-ray data from Peres et al (1998). The selection criteria for our sample are: a cooling flow greater than 100 solar masses per year, a redshift that places the H_2 emission line in one of the ava CFHTIR filters, and celestial availability. Our cooling flow rate cutoff of 100 solar masses per year was cl in light of the recent Chandra and ROSAT observations suggesting rates of a factor of 10 lower (McNa 2001). The three clusters that match our selection criteria are Abell 85, Abell 2319 and Abell 644. redshifts of our CFCs (z= 0.0521, 0.0564, and 0.0704) lie between those observed by Donahue et a 0.01756, 0.0852, and 0.1028). This is especially interesting in that this different sample of redshifts will e us to find trends currently unavailable due to an insufficient number of sources. We also anticipate a pro for next semester (2003A) to catch those CFCs with spring positions.

To date, most of our knowledge of cooling flows concerns the atomic and ionic gas components, which ger optical and X-ray emission. The proposed observations of these CFCs offer the promise of a greatly imp understanding of the molecular gas associated with the cooling flow phenomenon.

11. References *(1 page maximum)*:

Braine, J. and Dupraz, C. 1994, A&A 283, 407.
Bohringer, H. 2002, A&A 382, 804.
Donahue, M. et al 2000, ApJ 545, 670.
Edge, A.C. et al 1990, MNRAS, 245, 559.
Edge, A.C. 2001, MNRAS, 328, 762.
Fabian, A.C. 1994, Ann. Rev. AA 32, 277.
Falcke, H. 1998, ApJ 494, L155.
Jaffe, W. and Bremer, M.N. 1997, MNRAS 284, L1.
McNamara, B.R. 2001, from XXIst Moriond Astrophysics Meeting.
Peres, C.B. et al 1998, MNRAS 298, 416.

13. Technical Justification

(provide technical details of the proposed observations; justify the use of the CFHT, the requested instrument configura and the amount of telescope time requested: 1 page maximum):

Donahue et al (2000) found an H_2 1-0S(1) line flux of $3.92x10^{-15}$ erg s-1 cm-2 arcsec-2 in NGC (z=0.01756), or $3.92x10^{-18}$ W m-2 arcsec-2. The three clusters in our sample are Abell 85 (z=0.0 Abell 2319 (z=0.0564), and Abell 644 (z=0.0704). For Abell 2319, the H_2 1-0S(1) line is detected in th 2-1S(1) filter. For the other two clusters, the H_2 1-0S(1) line is detected in the K-continuum filter. I assume that the H_2 1-0S(1) line flux scales roughly as 1/z, as might be expected for filamentary emission calculate an expected H_2 1-0S(1) line flux of 1.32, 1.22, and $1.02x10^{-18}$ W m-2 arcsec-2, respectively.

For Abell 2319, the signal we want to detect in the H_2 2-1S(1) filter has a flux of $6.1x10^{-17}$ W m-2 arc um-2. Unfortunately, the H_2 1-0S(1) line also falls into the K-continuum filter so the continuum mus observed in a different filter — we choose Br-gamma. The continuum flux expected in the Br-gamma is $2.1x10^{-16}$ W m-2 arcsec-2 um-2 (surface brightness changes very little for these redshifts so we assume same value for all our clusters). As there is no sensitivity limit on the CFHT web pages for the H_2 2-1 filter, we assume the same limits as for the Br-gamma filter, i.e. 18.3 mag arcsec-2 for an extended so (5-sigma, 1000s) or $1.95x10^{-17}$ W m-2 arcsec-2 um-2. The integration time required to detect the H_2 1-0 emission with a S/N=5 in the H_2 2-1S(1) filter image (with continuum emission subtracted, thereby increa the noise by a factor of sqrt(2)) is 42m on-source for Abell 2319. The exposure time required in the Br-ga filter for continuum subtraction is the same as for the H_2 2-1S(1) filter, 42m.

For the other two clusters, we expect an H_2 line flux of $2.2x10^{-17}$ and $1.7x10^{-17}$ W m-2 arcsec-2 um-2 i K-continuum filter. The expected continuum fluxes in the CO filter are both around $2.1x10^{-16}$ W m-2 arc um-2. Again, there is no sensitivity limit on the CFHT web pages for the K-continuum filter so we assum same flux sensitivity limits as for the Br-gamma filter, divided by a factor of sqrt(3) to account for the l filter bandwidth. We find a 5-sigma, 1000s sensitivity in the K-continuum filter to be 18.9 mag arcsec-2 f extended source ($1.12x10^{-17}$ W m-2 arcsec-2 um-2). The integration time required to detect the H_2 1-0 emission with a S/N=5 in the K-continuum image (with continuum emission subtracted) is 2.8h on-sc for Abell 85. Separate observations in the CO filter to subtract the continuum emission require 8.5h for 85. Because of the lower expected flux from Abell 644, the integration times required for 5-sigma dete are prohibitively long. If we reduce our target to 3-sigma, we require 1.7h in K-continuum and 5.1h in

The total integration time required for all 3 clusters is 19.5 hours. Previous experience with CFHT-IR lea to believe that we will need exposure times of order 20s in order to avoid saturation. The additional over (bias, readout, saving data) is about 10s per integration, giving a 50% overhead, requiring 29.25 hours.

Allowing about 2 hours per night for standard stars and target acquisition, we might expect to have 10 h per night available. We therefore request 3 nights of telescope time.

14. Targets:

Object/Field	α	δ	Epoch	Mag/Flux	Comment
A85	00:41:50.8	-09:18:07.0	2000	15.7	Not same as CC
A644	08:17:25.5	-07:30:40.0	2000	16.2	Not same as CC
A2319	22:16:51.4	-10:48:35.0	2000	15.4	

15. General Target Information:

RA and DECs are the coordiates for the peak x-ray emmission. CC stands for Cluster Center.

16. Is this program conducted in relation with other observations (optical, radio, space)?

NO

17. How many additional nights or hours at CFHT would be required to complete this project? 0 nights

18a. Is an extension of the one-year proprietary period required? NO 18b. Proposed proprietary period? 12 mo

18c. If yes, justify the request for an extension:

19. Recent Allocations on CFHT and Other Telescopes:

Marleau, Welch, Tothill, and Edwards. Gemini South 8m telescope program GS-2001B-Q-12.
Welch and Sage. KPNO 12m telescope programs W-006, W-007. February 2002. 44 hours.
Welch and Sage. JCMT programs m01b-c04. December 2001 5 shifts.
Sage and Welch. NRAO 12m telescope program S-003. January 2001. 42 hours.

20. Publications Resulting from CFHT Observations *(only the 12 most recent contained in the database are displayed)*:

J.B. Hutchings and L. Edwards 2000, AJ, 119, 1100

Signature: signed via "POOPSY"

Appendix C:

Observing Proposals

Gemini Proposal

GEMINI OBSERVATORY

observing time request (HTML summary)

Semester: 2003A	**Partner reference:** Not Available	**PI time requested:** 24.0 hours
Gemini reference: Not Available	**Partner ranking:** Not Available	**PI minimum time requested:** 23.5 hours
Instruments(s):	**NTAC recommended time:** 0.0 nights	**PI future time requested:** 0.0 hours
Observing mode: queue	**NTAC minimum recommended:** 0.0 nights	**PI total from all partners:** 0.0 nights *(joint proposals)*
Time awarded: Not Available	**Proposal submitted to:** Canada	

Title:	**Molecular Hydrogen Spectroscopy of Cooling Flow Galaxies**
Principal Investigator:	**Francine Marleau**
PI institution:	Saint Mary's University, Department of Astronomy and Physics,Halifax,NS,B3H 3C3,Canada
PI status:	PhD/Doctorate
PI phone / fax / e-mail:	
Co-investigators:	

Abstract: *We wish to survey a sample of 5 cooling flows for near-infrared rovibrational lines of molecular hydrogen, using near-infrared spectroscopy. Cooling flows are produced by the cooling of the hot intracluster medium, but the molecular component and its excitation are poorly understood. By covering a range in redshift and cooling flow mass rate, we will look for trends in the H_2 flux, compare it with the optical and X-ray signatures of atomic and ionic gas, and elucidate the excitation mechanism of these lines.*

Science Justification

X-ray observations of nearby clusters of galaxies show sharp peaks, as dense gas in the centre of the cluster cools. This cool gas is then unable to support the outer part of the intracluster medium, which flows towards the centre of the cluster. The result is a long-lived stable `cooling flow' of gas into the centre of the galaxy cluster (see review by Fabian 1994). In the very central regions of these flows, the gas is expected to become molecular. Near-infrared rovibrational lines of H_2 have been detected

towards the central galaxies in a number of cooling flows (e.g. Falcke et al 1998, Donahue et al 2000), which is characteristic of molecular gas at temperatures of order 1000 K.

In general, this emission seems to be much too strong to be caused simply by the molecular cooling flow gas passing through this temperature range as it cools, emitting near-infrared lines; the inferred mass cooling rate from H_2 is much larger than that inferred from X-ray observations (Jaffe & Bremer 1997). Moreover, searches for CO emission from the molecular gas have found only small amounts (e.g. Edge 2001, Braine & Dupraz 1994). One explanation of this discrepancy is that the molecular gas, once formed, is reheated by some mechanism, such as shocks or reionisation of the gas by an AGN (Bohringer 2002) or a massive starburst in the central galaxy (Edge 2001). The H_2 emission could also be fluorescent in nature, due to the excitation of molecular gas by the ultraviolet radiation field from the AGN or early stars. Donahue et al (2000) give evidence on energetic grounds that the emission cannot be caused by shocks, but is more likely to be due to excitation by a young stellar population. However, there is no direct evidence to support this scenario, and the precise excitation mechanism by the radiation field is unclear. In addition, there are few detections of H_2 in the literature, so that there is little understanding of the systematic properties of H_2 emission in cooling flows - Do all cooling flows show H_2 emission? Does H_2 emission strength correlate with cooling flow emission or optical emission lines such as H-alpha? Does it correlate with redshift?

We propose a set of observations with two purposes - firstly to elucidate the excitation mechanism of the H_2 and secondly to act as a pilot survey of H_2 emission in cooling flows. The grism spectroscopy mode of FLAMINGOS is well-suited to these goals: the use of spectroscopy allows us to observe the H_2 emission lines over a wide range of redshift (which is not possible with narrow-band filters) and picks up the emission of several rovibrational transitions in the 2 micron wave band. Note that a pilot study has also been proposed with CFHT for semester 2002B to observe 3 cooling flow clusters at 2.12 microns with narrow-band filters. We will therefore have spectral and spatial information.

In order to study the excitation mechanism, we need to obtain the ortho/para ratio of molecular hydrogen, using odd and even transitions, e.g. 1-0S(1) and 1-0S(2). Gas that has been shocked will have an ortho/para ratio of 3, as set by the degeneracies, since it has been brought into equilibrium (e.g. Ramsay et al 1993). On the other hand, fluorescence-excited H_2 will retain the non-equilibrium ortho/para ratio with which it was formed, in the range 1-2. Furthermore, fluorescent emission should show lines in higher vibrational bands, e.g. H_2 2-1S(3). By carrying out spectroscopy, we will be able to obtain measurements of several transitions, allowing us to constrain the excitation mechanism directly.

We wish to obtain spectra towards 5 cooling flow clusters. The sample is taken from the B55 flux-limited sample of Edge et al (1990), with optical counterparts and further X-ray data from Peres et al (1998). Targets were carfully chosen so as not to overlap with the recent observations of Edge et al (2002). Our sample provides additional low mass accreation rate clusters that were ignored by the Edge survay. One of the targets has a low H-alpha detection, and as suggested by Wilman et al (2002), will help determine at what optical line streagth cooling flow clusters emit H_2.

To date, most of our knowledge of cooling flows concerns the atomic and ionic gas components, which generate optical and X-ray emission. The proposed spectroscopic observations of these clusters offer the promise of greatly improved understanding of the molecular gas associated with the cooling flow phenomenon, which is still poorly characterised and understood.

Attachments:

Name	Source	Type
Table of sources	soruce_table.txt	TEXT
References	references.txt	TEXT

Technical Justification

Edge et al (2002) found an H_2 1-0S(1) line flux of 10^-18 W m-2 arcsec-2 for many for many of thier cooling flow clusters at redshifts of about 0.01. Our sample comprises redshifts from 0.01 to 0.03. We assume that the H_2 1-0S(1) line flux scales as 1/z. Lines of para-H_2 are weaker than those of ortho- (e.g. Falcke et al 1998), so in order to derive an accurate ortho/para ratio, we need to be able to detect lines down to 10^-20 W m-2 arcsec-2.

FLAMINGOS has a quoted 5-sigma, 1-hour sensitivity of 17.56 mag arcsec-2, if the source is nodded along the slit direction (since these galaxies are small compared to the slit length, this can be done). The minimum observing time per target in the Queue mode is 1 hour. For a 5 sigma detection, our furthest target requires 5.8h integration time and our nearest source requires 2 hours integration time. Assuming 30 minutes setup time and 30% overheads, this gives 8.0 hours and 3.0 hours respectively. This will give adequate sensitivity for ortho and para-H_2 lines, and may also allow us to detect lines of higher vibrational transitions, which are expected in fluorescent emission. The sensitivity should also be satisfactory if the data are taken in non-optimum conditions (non-photometric conditions, high airmass, etc), as allowed by our observing constraints.

The total telescope time for the 5 programme sources is therefore 23.5 hours. Observing a standard star for flux calibration will add another 30 min (this is chiefly setup time, since only a few seconds' integration will be required). Our total time request is therefore 24 hours. If flux calibration observations are taken automatically, then the observation of UK IRT FS5 is not required, and the total time request is 23.5 hours.

Observation Details

Observation	RA	Dec	Brightness	Total Time *(including overheads)*
Abell1656	12:59:51.8	27:56:46	H2 1-0S(3) 18.02 arcsec-2	4.0 hours
GSC0199501971 (wfs)	13:00:17.806	27:57:19.73	12.04 mag	separation 5.77
observing conditions: Global Default		resources:		
MKW4s	12:06:37.7	28:09:57	H2 1-0S(3) 19.46 mag arcsec-2	6.0 hours

GSC0198800259 (wfs)	12:06:12.274	28:08:01.43	15.95 mag	separation 5.93
observing conditions: Global Default		resources:		
Abell3526	12:48:48.9	-41:18:44	H2 1-0S(3) 18.27 mag arcsec-2	2.0 hours
GSC0777900440 (wfs)	12:49:03.046	-41:23:30.73	14.66 mag	separation 5.48
observing conditions: Global Default		resources:		
Abell1060	10:36:43.2	-27:31:40	H2 1-0S(3) 18.50 mag arcsec-2	2.5 hours
GSC0664101452 (wfs)	10:36:20.381	-27:27:56.16	14.80 mag	separation 6.29
observing conditions: Global Default		resources:		
Virgo	12:30:49.0	12:23:35	H2 1-0S(3) 18.27 mag arcsec-2	2.0 hours
GSC0087700335 (wfs)	12:30:48.979	12:29:12.19	8.44 mag	separation 5.62
observing conditions: Global Default		resources:		
UKIRT FS5	01:54:34.65	-06:46:00.4	K 12.3	30.0 minutes
GSC0468800134 (wfs)	1:54:47.371	-6:50:53.66	15.35 mag	separation 5.82
observing conditions: Global Default		resources:		

Resources

Observing Conditions

Name	Image Quality	Sky Background	Water Vapor	Cloud Cover
Global Default	Any	Any	Any	70%

Scheduling Information:

Synchronous dates:

Optimal dates: 2002/9/29-2002/11/19
Reason: Celestial availabity of sources

Impossible dates: 2002/12/1-2003/1/31
Reason: Flamingos-I is available during August-November only

Additional Information

Keyword Category: Extra Galactic

Keywords: Cooling flows, Emission lines, Galaxy clusters

Publications:

- Rizza, E., Loken, C., Bliton, M., Roettiger, K., Burns, J.O., Owen, F.N. 2000, X-Ray and Radio Interactions in the Cores of Cooling Flow Clusters, AJ, 199, 21
- Loken, C., Melott, A.L., Miller, C.J. 1989, Massive Cooling Flow Clusters Inhabit Crowded Environments, ApJ, 520, L5
- Garasi, C., Loken, C., Burns, J.O., Roettiger, K. 1998, Numerical Simulations of Rotating Cooling Flows in Galaxy Clusters Environments, MNRAS, 298, 697

Allocations:

Reference	Time	% Useful	Comment
GS-2001B-Q-12	8.6 hours		Molecular Hydrogen Spectroscopy of Cooling-Flow Galaxies Note: no data were taken in spectroscopy mode with Flamingos-I in semester 2001B

Proposal Contents

References

- Allen et al, 2001, *MNRAS*, **324**, 877
- Arnaud, K., 1988, *Cooling flows in Clusters and Galaxies, Proceedings of the NATO Advanced Research Workshop*, Kluwer Academic Publishers, 31.
- Baker, K., et al., The Riddle of Cooling Flows in Galaxies and Clusters of Galaxies, Charlottesville, VA May 31- June 4, 2003
- Brauer, F., Sarazin, C.L., 2000, *ApJ*, **530**, 222
- Blanton, E., et al, 2001, *ApJ*, **558**, L15
- Blanton, E., The Riddle of Cooling Flows in Galaxies and Clusters of Galaxies, Charlottesville, VA May 31- June 4, 2003
- Bohrniger, H., Matsushita, K., Churazov, E., Ikebe, Y., Chen, Y. 2002, *A & A*, **382**, 804
- Braine, J., Dupraz, C. 1994, *A & A*, **283**, 407
- Carroll, B.W., Ostlie, D.A., 1996, *An Introduction to Modern Astrophysics*, Addison-Wesley Publishing Company, Inc., Reading
- Cowie, L.L., Hu, E.M., Jenkins, E.B., York, D. G. 1983, *ApJ*, **272**, 29
- Crawford, C.S., The Riddle of Cooling Flows in Galaxies and Clusters of Galaxies, Charlottesville, VA May 31- June 4, 2003
- David, L.P., et al., 2001, *ApJ*, **557**, 546.

- Donahue, M., Mack, J., Voit, G.M., Sparks, W. 2000, *ApJ*, **545**, 670
- Edge, A.C., 2001, *MNRAS*, **328**, 762E
- Edge, A.C., Wilman, R.J., Johnstone, R.M., Crawford, C.S. 2002, *MNRAS*, **337**, 49
- Eilek, J.A., Owen, F.N., 2002, *ApJ*, **567**, 202
- Ettori, S., Fabian, A.C., Allen, S.W., Johnstone, R. M., 2002, *MNRAS*, **331**, 635
- Fabian, A.C., 1994, *Annu. Rev. Astron. Astrophys.*, **32**, 277
- Fabian, A.C., 2000, *MNRAS*, **318**, L65
- Fabian, A.C., Mushotzky, R.F., Nulsen, P.E.J., Peterson, J.R. 2001, *MNRAS*, **321**, L20
- Fabian, A.C., et al. 2001, *MNRAS*, **321**, L33
- Fabian, A.C., The Riddle of Cooling Flows in Galaxies and Clusters of Galaxies, Charlottesville, VA May 31- June 4, 2003
- Fabian, A.C., Mushotzky, R.F., Nulsen, P.J.E., Peterson, J.R. 2003, *MNRAS*, **321L**, 20F
- Falcke, H., Rieke, M.J., Rieke, G.H., Simpson, C., Wilson, A.S., 1998, *ApJ*, **494L**, 155F
- Finoguenov, A., Jones, C., 2001, *ApJ*, bf 547L, 107F

- Flores, R. A., Quintana, H., Way, M. J., 2000, *ApJ*, **532**, 206
- Furusho T., et al, 2001, *PASJ*, **53**, 421
- Grenacher, L., Jetzer, Ph., Puy, D., 1999, *astro-ph*, **9911438**
- Gruber, Y. and Raphaeli, D., 2002, *ApJ*, **565**,977
- Heinz, S., Choi, Y.-Y., Reynolds, C.S., Begelman, M.C., 2002, *ApJ*, **569**, L79

  Houck, J.C., Davis, D.S., Wise, M.W., *Two Years of Science with Chandra*, Abstracts from the Symposium held in Washington, DC, Sept. 5-7, 2001
- Jaffe, W., Bremer M.N. 1997, *MNRAS*, **284**, L1
- Jaffe, W., Bremer, M.N., van der Werf, P.P. 2001, *MNRAS*, **324**, 443
- Johnstone, R., *The Epoch of Galaxy Formation*, Proceedings of the NATO Advanced Research Workshop, held in Durham, U.K., July 18-22, 1988
- Kempner, J.C., and Sarazin, C.L., *Two Years of Science with Chandra*, Abstracts from the Symposium held in Washington, DC, Sept. 5-7, 2001
- Krawczynski, H., 2002, *ApJ*, **569**, L27
- Lebofsky, M.J., 1981, *ApJ*, **245**, L59
- Machacek, M.E., Bautz, M.W., Canizares, C.G., G.P., 2002, *ApJ*, **567**, 188
- Markevitch, M., The Riddle of Cooling Flows in Galaxies and Clusters of Galaxies, Charlottesville, VA May 31- June 4, 2003

- Markevitch, M., et al., 2000, *ApJ*, **541**, 542
- McNamara, B.R., Wise, M., Sarazin, C.L., Jannuzi, B.T., 1996, *ApJ*, **466L**, 9M
- McNamara, B.R., et al, 2001, *ApJ*,**562**, 149
- Navalainen, J., 2001, *A&A*, **369**, 459
- Peres, C.B., Fabian, A.C., Edge, A.C., Allen, S.W., 1998, *MNRAS*, **298**, 416P
- Peterson, J.R., et al. 2001, *A&A*, **365**, L104
- Pinkney J., et al. 1996, *ApJ*, **468**, L13
- Salomé, P. and Combes, F., The Riddle of Cooling Flows in Galaxies and Clusters of Galaxies, Charlottesville, VA May 31- June 4, 2003
- Sarazin, C. L., 1988, *Cooling flows in Clusters and Galaxies, Proceedings of the NATO Advanced Research Workshop*, Kluwer Academic Publishers, 1
- Schmidt, R.W., Allen, S.W., Fabian, A.C., 2001, *MNRAS*, **327**, 1057
- Sodre, L., Proust, D., Caelato, H.V., et al. 2001, *A & A*, **377**, 428
- Srinivasan, R., Mohr, J.J., 2001, AAS meeting, 199, # 100.14
- Stanford, S. A., Eisenhardt, P. R., and Dickinson, M. 1995, *ApJ*, **450**, 512
- Stocke, J., Lewis, A., 2000, AAS meeting, 197, # 106.02
- Tamura, T et al, 2001, *A&A*, **365**, L87

- Tucker, W.H., Rostner, R., 1983, *ApJ*, **267**, 547
- Vikhlinin, A., Markevitch, M., Murray, S.S., 2001, *ApJ*, **551**, 160
- Voit, M., The Riddle of Cooling Flows in Galaxies and Clusters of Galaxies, Charlottesville, VA May 31- June 4, 2003
- White, D.A., 2000, *MNRAS*, **312**, 663
- Wilman, R.J., Edge, A.C., Johnstone, R.M., Crawford, C.S., Fabian, A.C., 2000, *MNRAS*, **318**, 1232
- Wilman, R.J., Edge, A.C., Johnstone, R.M., Fabian, A.C., Allen, S.W., Crawford, C.S., 2002, *MNRAS*, **337**, 63